



Electrochemical aptasensors based on the gold nanostructures

Masoud Negahdary

Nanomedicine and Nanobiology Research Center, Shiraz University of Medical Sciences, Shiraz, Iran

ARTICLE INFO

Keywords:

Aptasensors
Diagnostic aptamers
Bioelectrochemistry
Gold (Au) nanostructures
Aptamer-based biosensors
Nanobiosensors

ABSTRACT

Electrochemical aptasensors as novel diagnostic tools have attracted sufficient research interest in biomedical sciences. In this review, recent leading trends about gold (Au) nanostructures based electrochemical aptasensors have been collected, reviewed, and compared. Here, the considered electrochemical aptasensors were categorized based on the analytes and diagnostic techniques. Pharmaceutical analytes and biomolecules were reviewed in a separate section consisting of a variety of antibiotics, analgesics, and other biomolecules. Various aptasensors have also measured toxins, ions, and hazardous chemicals, and the findings of them have also been reviewed. Many aptasensors have been designed to detect different disease biomarkers that will play an essential role in the future of early diagnosis of diseases. Pathogen microorganisms have been considered as the analyte in several designed electrochemical aptasensors in recent researches, and their results have been reviewed and discussed as another section. Important aspects considered in the review of the mentioned aptasensors were the type of analyte, features of the aptamer as the biorecognition element, type of Au nanostructures, diagnostic technique, diagnostic mechanism, detection range and the limit of detection (LOD). In the last section, an in-depth analysis has been provided based on the crucial features of all included aptasensors.

1. Introduction

The rapid development of technology in the design of biomedical tools, especially biosensors, provided optimized diagnostics. Biosensors have been widely used due to several key advantages, including simple and inexpensive design, portability, and rapid and accurate detection of the analyte(s) [1–3]. Each biosensor consists of three main elements, including the biorecognition element, the signal transducer, and the detector [4,5]. The most important biorecognition elements that have recently been used in the design of biosensors are included antibodies [6], aptamers [7–12], peptides [13,14], and biological polymers [15] that have been developed against various analytes to provide specified diagnostics. In this review, electrochemical aptasensors have been investigated due to their importance and applications, where the signal transducer reports electrochemical events before the presence of an analyte and in existence it as electrical signals to the detector (in most cases a monitor equipped with a potentiostat/galvanostat device) [16]. Mostly, the signal transducers are Au, glassy carbon, and carbon paste electrodes. Also, these electrochemical biosensors usually detect analytes by several techniques such as cyclic voltammetry (CV) [17], differential pulse voltammetry (DPV) [18], electrochemical impedance spectroscopy (EIS) [19], square wave voltammetry (SWV) [20], photoelectrochemical (PEC) [21] and electrochemiluminescence (ECL) [22]. Analytes in biosensors consist of a wide range of organic and

inorganic materials that accurate and rapid detection of them has particular importance. The most important analytes in biosensors include biomarkers of various diseases [13,23–37], pathogenic microorganisms [38–41], toxins, and hazardous chemicals [42–55], drugs, and biological molecules [56–62]. Whatever the biorecognition element be more specific and affinitive against the analyte, the designed biosensor will have higher selectivity and stability. Therefore, the selection and using the most optimal biorecognition element against the analyte are crucial. Aptasensors are a type of biosensors in which their biorecognition element is an aptamer [63–65]. The aptamers are oligonucleotides (mostly DNA and RNA) with 20–80 nucleotides that are produced with the systematic evolution of ligands by exponential enrichment (SELEX) method [66,67]. Aptamers have many advantages over other biorecognition elements used in the structure of biosensors (especially antibodies), and due to this reason, aptasensors have been extensively developed to detect various analytes [64,68]. Important advantages of aptamers as the biorecognition element in the structure of biosensors include a high affinity against target molecules that provided them to be folded into a three-dimensional structure and be specifically and tightly attached to their targets. The aptamers selected due to their high affinity against a wide range of analytes (micro and macromolecules) can be used in the detection and quantification of substances such as metal ions (Hg^{2+} , Pb^{2+} , etc.), small organic molecules (amino acids, ATP, antibiotics, vitamins, narcotics, and other

E-mail addresses: masoudnegahdary@ssu.ac.ir, masoudnegahdary@ssu.ac.ir.

<https://doi.org/10.1016/j.talanta.2020.120999>

Received 12 February 2020; Received in revised form 29 March 2020; Accepted 1 April 2020

Available online 06 April 2020

0039-9140/ © 2020 Elsevier B.V. All rights reserved.

drugs), macromolecules (such as peptides, proteins, growth factors, dyes, toxins, pathogens, and biomarkers), and microorganisms (such as bacteria and viruses) [69,70]. Aptamers are substantially smaller than antibodies and proteins [64,68]. Other advantages of aptamers include temperature stability, easy transport, and inexpensive synthesis, as well as low immunogenicity and toxicity [71,72]. One of the most useful properties of aptamers is their functionality at the 5' and 3' end with various functional groups such as thiol, amine, biotin, and so on [73,74]. The purpose of aptamer functionalization is to establish specific binding on the surface of the signal transducer or other components of the biorecognition element as well as to increase the stability of aptamer function (e.g., increased resistance against nucleases) [73–75]. Nanostructures are materials that their size is smaller than 100 nm in at least one dimension. Reducing the size of a material to the nanoscale causes significant changes in the physical and chemical properties [76,77]. As the surface area to volume ratio is increased, the electrochemical, optical, thermal, mechanical, and chemical reactivity properties of the materials are changed. Different synthesis methods, synthesis compounds as well as synthesis conditions lead to the production of nanostructures with the desirable sizes and morphologies [78,79]. Au is a yellow, soft, and neutral metal with a melting temperature of 1068 °C. This metal exhibits special properties at the nanoscale sizes that have made it an important metal in numerous nanotechnology applications and products [80,81]. Au nanostructures have been widely used in biomedical studies and especially in biosensor design owing to their high biocompatibility, ease of synthesis, controllability of synthesis, and the stability in the synthesis process and application [82]. Au nanostructures have been used in the biosensor structure mainly as a deposited layer on the surface of the signal transducer or as a conjugated form with the biorecognition element to enhance the diagnostic sensitivity obtained from the increased surface area [83,84]. In this review, the most recent and leading Au nanostructured based electrochemical aptasensors are investigated. In section 2, aptasensors for drug detection, especially antibiotics as well as biomolecules, have been studied. In section 3, the aptasensors for toxins detection, hazardous metal ions, and chemicals are evaluated. In section 4, aptasensors for diagnostic biomarkers (especially cancer biomarkers) and for evaluating the prognosis as well as the progression of various diseases are reviewed. In section 5, aptasensors for the detection of pathogenic microorganisms are investigated. In section 6, as the final section, the main features of evaluated aptasensors have been analyzed and categorized.

2. Electrochemical aptasensors based on the Au nanostructures for diagnosis of drugs and biomolecules

2.1. Aptasensors for diagnosis of drugs

2.1.1. Aptasensing of antibiotics

Antibiotic resistance is one of the most significant challenges of today's society. The improper use of a wide range of antibiotics in the prevention of infectious diseases of animals, poultry, and humans has resulted in a less effective or even ineffective role of these drugs [85]. Oxytetracycline (OTC) is a broad-spectrum bacteriostatic antibiotic that binds to the bacterial 30S ribosomal subunit and inhibits the binding of aminoacyl-tRNA to this subunit, thereby preventing protein synthesis and ultimately growth [86]. OTC can be used against gram-positive bacteria such as *Staphylococcus*, *Streptococcus*, and gram-negative bacteria such as *Pasteurella*, *E. coli*, *Haemophilus*, *Mycoplasma*, *Rickettsia*, *Chlamydia*, and *Spirocytes*. World Health Organization (WHO) considered a level residue limit of 0.1 mgL⁻¹ for OTC residues in human nutrition. OTC, as an antibiotic, was detected by an electrochemical aptasensor equipped with Au nanoparticles (NPs) [87]. First, a thin film Au electrode was manufactured from an Au film on a polycarbonate substrate. In this screen-printed electrode, the Au area was considered as the working electrode. At the next step, carboxylated

multi-walled carbon nanotubes (cMWCNTs) and Au NPs were prepared and mixed by a procedure, and then a thiol functionalized complementary strand of Apt (cDNA) was added to obtain cMWCNTs/Au NPs/cDNA conjugated form. On the other side, a thiolated aptamer was dropped and immobilized on the surface of the working electrode for 1 h. Subsequently, cMWCNTs/Au NPs/cDNA solution was dropped on the surface of the working electrode and immobilized during 150 min. Finally, thionine (Thi) as the signal probe was added and attached to cDNA, and the prepared aptasensor was applied for the determination of OTC in various concentrations. In the absence of OTC, hybridization occurred between aptamer and cDNA where the Thi was at a maximum level. However, in the presence of OTC, due to a higher affinity between the aptamer and OTC, the aptamer captured OTC and the most of cMWCNTs/Au NPs/cDNA structure containing Thi was released, and this event was led to decrement the DPV currents along with the increment of OTC concentrations. This signal-off aptasensor could detect OTC in a linear range from 1×10^{-13} - 1×10^{-5} g mL⁻¹, and the reported LOD was 3.1×10^{-14} g mL⁻¹. In another research, kanamycin (KAN) and streptomycin (STR) as two essential aminoglycoside antibiotics were detected concurrently by an electrochemical aptasensor [59]. The use of these antibiotics also has some side effects. Cochlear injuries, liver damage, renal toxicity, magnesium depletion, especially in long-term use of medication, pseudomembranous colitis, as well as hypersensitivity reactions and oral paresthesia are potential complications [88]. The residue limits for KAN and STR in milk is 150 µg kg⁻¹ and 200 µg kg⁻¹, respectively. In this research, the transducer was a screen-printed carbon electrode and modified with carbon nanofibers and the ordered mesoporous carbon (OMC)-Au NPs to improve the sensitivity. At the next step, 1-Ethyl-3-(3-dimethyl aminopropyl) carbodiimide (EDC)/N-hydroxysuccinimide (NHS) was added on the surface of the electrode to provide an activated carboxyl group. Afterward, two complementary amine-functionalized DNA strands were immobilized on the surface of the working electrode. The immobilization process was performed via an amide bond (CO-NH) between the carboxyl group of EDC/NHS-OMC-Au NPs and the amine group of complementary DNA strands. Then, the aptamers were labeled with CdS (prepared from Cd(NO₃)₂ and Na₂S) and PbS (prepared from Pb(NO₃)₂ and Na₂S) as signal probes; CdS was used for KAN aptamer, and PbS was used for STR aptamer. These aptamers were added on the surface of the working electrode and applied to provide the hybridized structures with complementary DNA strands in the absence of the desired antibiotics. Finally, the prepared aptasensor was applied for the detection of the various concentrations of KAN and STR. Here, the biorecognition elements were two amine-functionalized aptamers with the highest affinity against KAN and STR antibiotics. In the presence of KAN and STR, due to the higher affinity between the aptamer and analyte, a conformation change occurred, and aptamers were released from complementary DNA strands and captured the related analyte. The released aptamers in the electrolyte solution containing ferro/ferrocyanide as the redox marker was led to create the Cd²⁺ and Pb²⁺ ions along with the various concentrations of KAN and STR; this phenomenon established the DPVs with changes in peak currents. This aptasensor could detect these antibiotics in a linear range from 0.1 to 1000 nM while the LOD for KAN and STR was 87.3 pM and 45 pM, respectively. In another research, Penicillin G, as a usual antibiotic, was diagnosed by an impedimetric aptasensor [61]. Here, a pencil graphite electrode (PGE) was applied as the working electrode and modified with a nanocomposite containing the reduced graphene oxide (rGO) and Au NPs to provide a larger active surface area and enhance the sensitivity. In the first step, the PGE was modified with rGO and Au NPs, respectively. Subsequently, a high-affinity thiol-functionalized aptamer was used as the biorecognition element and immobilized on the surface of the working electrode. The designed aptasensor was applied for detection Penicillin G, and the changes of charge-transfer resistance (Rct) between the aptasensor and analyte was considered as a quantitative value for measurement. In the presence of the analyte, in

order to the higher affinity between the aptamer and analyte, reaction sites of aptasensor were captured by the analyte molecules, and redox molecule positions were changed; this event was led to increasing the R_{ct} ; by increasing the concentrations of analyte, the R_{ct} values were also increased regularly. This aptasensor was able to detect Penicillin G in a dynamic range from 1.0 fM to 10 μ M, and the obtained LOD was about 0.8 fM.

2.1.2. Aptasensing of anti-inflammatory pain relievers (ibuprofen)

Anti-inflammatory pain relievers, such as ibuprofen, are known as nonsteroidal anti-inflammatory drugs (NSAIDs). By blocking the effect of cyclooxygenase, ibuprofen reduces the production of a chemical termed prostaglandin (responsible for pain and inflammation in the affected area) [89]. So, pain and inflammation are reduced by inhibition of cyclooxygenase enzyme and reduced prostaglandin production. Ibuprofen has some side effects as well; gastrointestinal discomfort such as nausea, diarrhea, and occasionally bleeding ulcers may occur. Other side effects include allergic reactions, especially angioedema, bronchospasm, cutaneous rash, as well as headaches, dizziness, and hearing disorders such as tinnitus. In a research, an electrochemical aptasensor was presented for the determination of various concentrations of ibuprofen [90]. Here, a glassy carbon electrode (GCE) was applied as the working electrode in the three-electrode system. At the next step, the working electrode was modified with nitrogen-doped graphene quantum dots (NGQDs) and Au NPs, respectively. Then, the working electrode modified with Au NPs@N-GQDs nanocomposite was obtained. Afterward, an amine-functionalized capture aptamer was immobilized on the surface of the working electrode. In this step, a covalent Au-amine bond was created between Au NPs and 3' end of amine-functionalized capture aptamer. Finally, a specific ibuprofen aptamer was added and hybridized with the capture aptamer; the prepared aptasensor applied for determining the analyte. One of the substantial advantages of this research was applying riboflavin (vitamin B₂) as a green redox marker that is able for oxidation in negative potential values; working in this potential range is very applicable to remove the most of interfering effects. DPVs and CVs measurements were followed in an electrolyte solution containing riboflavin, NaCl, and phosphate buffer, while the EIS measurements were followed in the presence of ferro/ferricyanide as the redox marker. The detection mechanism was based on measuring the R_{ct} changes in the absence and presence of ibuprofen. In the presence of the analyte, the hybridized structure between the capture aptamer and ibuprofen aptamer was broken, and the aptamer attached to ibuprofen molecules with a high affinity. This event increased the R_{ct} due to the created space restriction against redox molecules and transducer and also decreased the electrochemical peak currents along with the higher concentrations of the drug. The linear detection range of this signal-off aptasensor was from 10^{-7} to 200 nM, and the LOD calculated as 33.33 aM.

2.1.3. Aptasensing of addictive drugs (cocaine)

Cocaine is a white, soft, translucent, crystalline powder, and with a bitter flavor extracted from plant leaves called "Erythroxylon Coca", a native plant of South America. It is widely used in medicine for topical anesthesia but is unauthorized for non-medical use worldwide and has been recognized for its numerous physical and psychological complications [91]. Cocaine is one of the most potent stimulant substances that directly affect the brain and creates a high euphoria. Cocaine is the most dangerous and addictive drug in the world that is only used a few times to cause severe dependence. In addition to addiction, poisoning with this substance can cause hallucinations and increase the body's vital activities such as heart rate and respiratory rate, hypertension, and increase body temperature. Other than the mentioned complications, heart attack, and stroke, leading to coma and death are common. In a research, Tavakkoli et al., reported an electrochemical aptasensor for diagnosis of cocaine [92]. An Au electrode was considered as the working electrode in a three-electrode system. This Au electrode was

converted to a nanoporous (50 ± 10 nm) Au electrode via oxidizing the Au surface with phosphate buffer at a potential of 3 V and then reduces the surface to metallic Au by immersing in ascorbic acid, respectively. At the next step, a specific aptamer sequence was immobilized on the surface of the working electrode. The applied aptamer was modified with 2,5-dihydroxybenzoic acid (DHBA) as the responsive probe and also functionalized with amine and disulfide groups. This aptamer was functionalized with a disulfide group from 5' end that attached to the nanoporous Au surface through the Au-S bond. On the other side, 3' end was functionalized with amine and conjugated (amide bond: amine group of aptamer and carboxyl group of DHBA) with DHBA. It should be noted that the disulfide group was reduced to the thiol group before immobilization of aptamer, and the carboxyl group of DHBA was activated with EDC/NHS before conjugation. The mechanism of detection was based on the distance of DHBA from the surface of the working electrode. In the absence of cocaine, aptamer was located in a far distance from transducer while in the presence of this drug, due to a high affinity between aptamer and analyte, aptamer conformation changed (analyte captured) and the DHBA located in a closer distance from the transducer. Decrement of the distance between the DHBA and surface of the working electrode increased the peak currents along with the concentration of analyte regularly. This signal-on aptasensor could determine cocaine in a linear range from 0.05 to 35 μ M, while the LOD was 21 nM.

2.2. Aptasensors for diagnosis of biomolecules

2.2.1. Aptasensing of biomaterials (vanillin)

Vanillin is a widely used edible spice and has a specific flavor that is either extracted from vanilla beans or synthesized in-vitro. Mostly, this biomaterial is produced using propylene glycol and other additives [93]. Vanillin can also be made from clove oil, wood pulp, or coal tar. The effect of vanillin on the nervous system and the human brain reduces fear and depression. The concentration of vanillin in foods should not be more than 100–250 ppm. Side effects of vanillin include headaches, skin rashes, malignancy, and kidney and liver toxicity. In a research, vanillin was detected by a ratiometric electrochemical aptasensor [62]. ZIF-8 is considered as one of the metal-organic frameworks (MOFs) with excellent thermal and chemical stability that applied by Sun et al. Poor electrical conductivity is a leading challenge during using of MOFs. In order to improve the electrical conductivity, ZIF-8 was synthesized and used as a composite form in the presence of ketjen black (KB)/ferrocene (Fc). KB is a type of carbon black. In order to synthesize the Fc-KB/ZIF-8 composite, 2-methylimidazole, Fc and KB were added in a methanol solution, respectively. Afterward, Zn (NO_3)₂·6H₂O was added to a methanol solution. Fc was doped into ZIF-8 and used as the reference signal producer. Here a GCE was applied as the working electrode and initially modified with Nafion as a cross-linker. Then, Fc-KB/ZIF-8 composite was dropped on the surface of the working electrode. Afterward, the surface of a GCE was modified with Au NPs through an electrodeposition process. In the last step, a thiolated aptamer sequence was immobilized on the surface and built the Au-S bonding with Au NPs (Fig. 1). This aptasensing platform was applied for the quantitative diagnosis of vanillin. In the presence of vanillin, this edible spice was captured by aptamer strands due to the high affinity between the aptamer and analyte, and the peak currents were increased along with the concentration; but, the peak currents related to Fc were unchanged. The ratio between the peak currents of vanillin and Fc was used for the sensitive determination of vanillin. This signal-on aptasensor could detect the vanillin in a linear range from 10 nM to 0.2 mM, and the obtained LOD was about 3 nM.

2.2.2. Aptasensing of essential proteins (lysozyme)

Lysozyme is an essential protein with a molecular weight of approximately 14.3 kDa that is present in microorganisms, plants, animals, and humans. Changes in the levels of this protein can be used as a

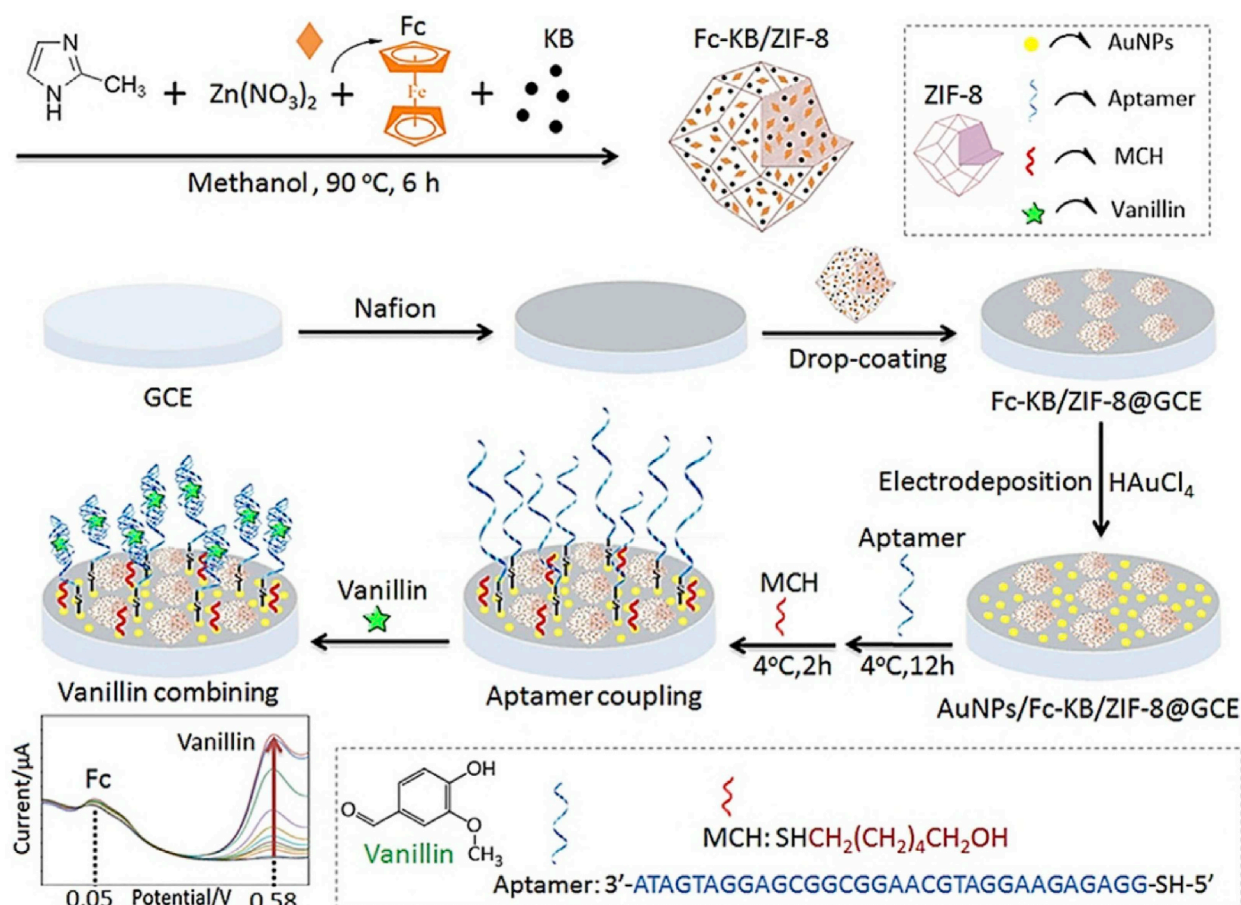


Fig. 1. Designing a ratiometric electrochemical vanillin aptasensor; License Number: 4715290970263.

biomarker for the diagnosis of various diseases such as cancers, AIDS, oral infection, atherosclerosis, malaria, and hyperglycemia [94,95]. A research has been introduced based on the design of an electrochemical aptasensor for the diagnosis of lysozyme [96]. First, a carbon nanotube paste electrode as the working electrode was prepared through a mixture containing 80% (w/w) carbon nanotubes and 20% paraffin. Then, the carbon nanotube paste electrode was modified with Au NPs (diameter: 13 nm). Subsequently, the thiolated complementary DNA sequence (c-DNA) was immobilized on the surface of the working electrode. At the next step, lysozyme binding aptamer (LBA) was added on the surface of the working electrode and hybridized with c-DNA. Finally, ethidium bromide (EB) molecules as a photosensitization tag were added to double-strand hybridized DNA structure, and the prepared aptasensor was applied for the diagnosis of lysozyme. In the presence of lysozyme molecules, due to the high affinity of LBA against the analyte, the double-strand hybridized DNA structure was broken, and LBA captured the analyte based on the conformation change. This phenomenon was led to the release of EB molecules, and the photosensitization event missed. At this time, c-DNA strands with a negatively-charged status were remained on the surface at a maximum amount and changed the electrochemical behavior of the working electrode against the redox marker. This signal-off aptasensor was able to determine the analyte in a range from 10 pM to 1 μM, and the LOD was 2 pM.

2.2.3. Aptasensing of hormones

17β-Estradiol (E2) is one of the most important and the primary female sex steroid hormones secreted by the premenopausal ovary. This biomolecule plays an essential role in the endocrine system, cardiovascular system, metabolism of fats, and health of the brain;

determining its concentration is also vital in the diagnosis of some diseases. It also has therapeutic roles in postmenopausal estrogen replacement and Alzheimer's disease [97]. In a research, E2 was determined by an electrochemical aptasensor [98]. Initially, a nanocomposite containing Au NPs (size: ~3 nm), Thi, and MWCNTs was synthesized and applied for modification of the surface of a GCE (as the working electrode). Then, the modified electrode was immersed in a solution containing a thiolated aptamer as the biorecognition element. After immobilization of aptamer on the surface of the GCE by Au-S covalent bond, the prepared aptasensor was applied for the diagnosis of E2. Here, Thi was used as a cationic phenothiazine dye for electrochemical measurements. In the absence and presence of E2, the electron transfer rate between the electrolyte and transducer was changed. In the presence of E2 molecules, peak currents of Thi were decreased, and the peak currents of E2 were increased along with increasing the concentration of the analyte. The ratio between the decreased and increased electrochemical signals was used for determination the E2. This ratiometric aptasensor was detected E2 in a linear range from 12 pM to 60 nM, and the reported LOD was 1.5 pM. Insulin is a hormone secreted from the pancreatic islet beta cells, and its primary role is to control blood sugar levels. Increased blood glucose level is the most key physiological regulator for insulin secretion. In this pathway, specific glucose receptors in beta cells stimulate insulin secretion when blood glucose increases [99]. Insulin facilitates the entry of blood glucose into the cells, where the sugar either burns and produces energy or is stored. Abnormal concentrations of insulin can be a sign of a variety of metabolic, genetic, and some cancers. In a research, a dual-signaling ratiometric electrochemical aptasensor for diagnosis of insulin was designed [100]. First, a thiolated aptamer strand (termed as DNA2) was conjugated with Au NPs and created DNA2@Au NPs structure;

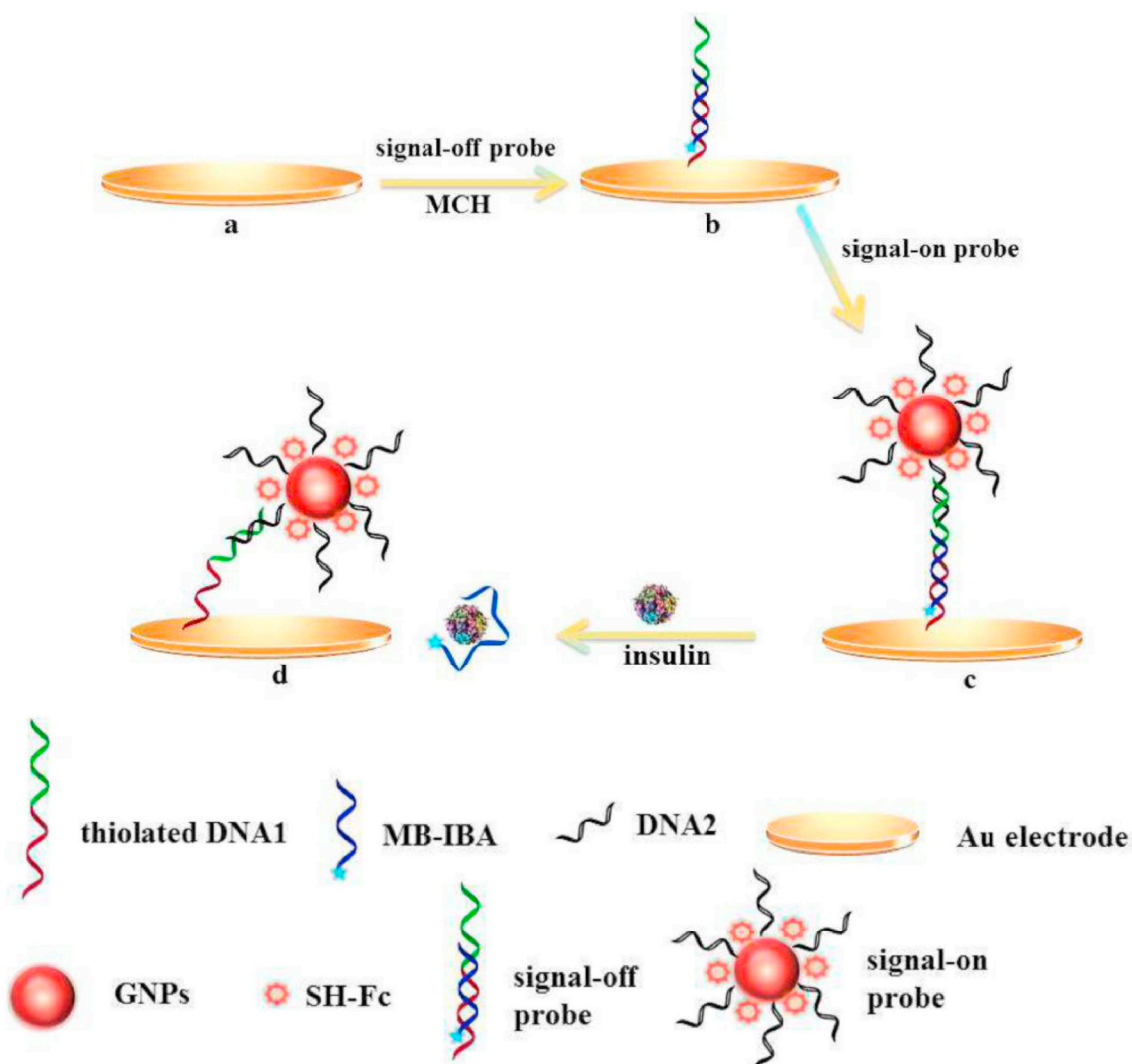


Fig. 2. Schematic presentation of a dual-signaling ratiometric electrochemical aptasensor for diagnosis of insulin; License Number: 4797710220870.

subsequently, Fc was added, and DNA2Fc@Au NPs was prepared. On the other side, another thiolated aptamer (termed as mDNA) was mixed and hybridized with a methylene blue (MB)-modified insulin-binding aptamer (IBA) and established a double-strand structure (mDNA@MB-IBA). Here, an Au electrode was used as the working electrode, and a solution containing mDNA@MB-IBA was immobilized on the surface of it; in the next step, DNA2Fc@Au NPs was added on the surface of electrode and mDNA was hybridized with DNA2 and an aptasensor with a specific structure (DNA2Fc@Au NPs/mDNA@MB-IBA/Au electrode) was fabricated (Fig. 2). In fact, DNA2Fc@Au NPs/mDNA@IBA/Au electrode assembly was used as a signal-on aptasensor, and DNA2@Au NPs/mDNA@MB-IBA/Au electrode assembly was used as a signal-off aptasensor. Fc and MB were used as the signal producer. In the absence of insulin, based on the Fc location in a far distance from the surface of the electrode, the associated peak current was in minimum, while the MB was located in a close location against the surface of the electrode and created a strong electrochemical signal. In the presence of insulin, a found high affinity between MB-IBA, and analyte changed the conformation of MB-IBA and this structure released from the surface of the electrode and captured the analyte. This event confirmed that the hybridized structure of aptamers (DNA2/mDNA) was broken, and DNA2Fc@Au NPs structure was located in a near position from the surface of the working electrode. So, in the presence of the analyte, the electrochemical signal of MB reduced, and the electrochemical signal of

Fc increased. The found electrochemical changes were related to the level of insulin and provided a quantitative method for the diagnosis of insulin via comparing the peak currents of MB and Fc. This aptasensor was able to detect insulin in a linear range from 10 pM to 10 nM, and the found LOD was 0.1 pM.

Recent designed electrochemical aptasensors based on the Au nanostructures for diagnosis of drugs and biomolecules have been collected and presented in Table 1.

3. Electrochemical aptasensors based on the Au nanostructures for diagnosis of toxins, metal ions and chemical compounds

Aflatoxin is a dangerous fungal toxin produced by *Aspergillus flavus*, *Aspergillus parasiticus*, *Aspergillus nomius*, and *Aspergillus tamaritii* in the presence of humidity and warm weather, and lack of proper storage conditions [116]. There are more than twenty types of aflatoxins, but the four main types are G₁, G₂, B₁, and B₂. Aflatoxins M₁ and M₂ are the hydroxylated metabolites of aflatoxins B₁ and B₂, and the most crucial metabolite is aflatoxin M₁. Dangerous side effects of this toxin are including inhibition of protein synthesis, mutagenesis, teratogenesis, carcinogenesis, and adverse effects on the liver, colon, kidney, lung, brain, and immune system. As an example, the maximum allowed residue level for this toxin in milk and infant formula are 50 ng kg⁻¹ and 25 ng kg⁻¹, respectively. In a research, aflatoxin M₁ as

(continued on next page)

(continued on next page)

Table 1 (continued)

Type of analyte	Aptamer sequence	Type of Au nanostructure	Detection technique	Detection range	LOD	Ref.
Homocysteine	5'-SH-(CH ₂) ₆ -ACCA GCAC ATTG GATT ATAC CAGC TTAT TCAA TTCA CAGC TATG TCCT ATAC CAGC TTAT TCAATT-3'	Au NPs	DPV	0.05–20.0 μ M	0.01 μ M	[114]
Sialic acid	5'-TCCCTACGGCGCTAACCGATAGGTGTAGCGTGGGGCACATGTTGGCGCCACCGGTGC TACAAAC-3'	Au nanodendrites	DPV	1.1–440 μ M	60 nM	[115]

a type of mycotoxins was detected by an electrochemical and Au NPs-based aptasensor [43]. Here, a screen-printed Au electrode (DRP-C220BT) was used as the transducer, and then a hairpin-shaped thiol-functionalized aptamer was immobilized on the surface of it. Afterward, the aflatoxin M₁ as an analyte was incubated on the surface of a screen-printed Au electrode. On the other side, a complementary strand (CS) was prepared and conjugated with Au NPs through the Au-S covalent bond. Then, CS-AuNPs added on the electrode, and subsequently, MB as the redox marker was added, and the associated electrochemical behavior of the aptasensor was followed via the DPV technique. In the absence of aflatoxin M₁, the aptamer was in a hairpin-shaped structure and as an unhybridized form with CS- AuNPs that a low amount of MB molecules could be accumulated on the surface of the screen-printed Au electrode; this event was led to provide a weak electrochemical DPV signal. Nevertheless, in the presence of aflatoxin M₁, due to a high affinity between aptamer and aflatoxin M₁, the hairpin-shaped structure of the aptamer was changed and provided a condition for successful hybridization with CS- AuNPs. In this status, when MB was added, an electrostatic interaction occurred that led to a massive accumulation of MB molecules on the surface of the electrode. This event was led to provide a strong electrochemical DPV signal along with the concentration of the analyte. This signal-on aptasensor was able to detect aflatoxin M₁ in a dynamic range from 2 to 600 ng L⁻¹, and the found LOD was equal to 0.9 ng L⁻¹. Ochratoxin A (C₂₀H₁₈O₆NCl) is one of the most critical mycotoxins and is produced by some *Penicillium* and *Aspergillus* species. This toxin has a potential risk to human health due to its carcinogenic, immunotoxic, teratogenic, mutagenic, and nephrotoxic effects. In a research, an electrochemical aptasensor has been introduced for specific determination of ochratoxin A [50]. This aptasensor was designed based on a nanocomposite (poly (3,4-ethylene-dioxy thiophene)/Au NFs/graphene oxide sponge) as the signal amplifier. In a review, we followed the applications of NFs in biomedicine [117]. Here, as the first step of electrode modification, the GCE was modified with graphene oxide sponge and then poly (3,4-ethylenedioxy thiophene)/Au NFs were added and attached on the graphene oxide sponge through π - π stacking interaction. The increased surface area of a modified GCE with the mentioned nanocomposite was applied for immobilization of a thiol-functionalized aptamer; the immobilization process was performed using the Au-S covalent bond. In the absence of ochratoxin A, the rate of electron transfer was at the maximum level and let to create an electrochemical signal with a specific peak current. In the presence of the analyte, due to a high affinity between aptamer and analyte, the aptamer's conformation changed and could capture the analyte. The captured analyte molecules reduced the conductivity between the redox marker and the transducer; this phenomenon was led to reducing the peak current related to each concentration of the analyte. This signal-off aptasensor was able to determine the analyte in a linear range from 0.01 to 20 ng L⁻¹ while the LOD was reported as 4.9 pg L⁻¹. Zearalenone (ZEN) is an estrogenic mycotoxin produced by several species of *Fusarium* fungi and has received particular attention due to its strong estrogenic effects. This toxin causes reproductive disorders in animals and, eventually, steroid disorders in humans. The allowed range of this toxin is 50 ng g⁻¹. Also, fumonisin B1 (FB1) is another mycotoxin produced by *Fusarium verticillioides* and causes nerve damage, esophageal cancer, and liver and kidney disease. The allowed range of this toxin is 4×10^2 to 4×10^3 μ g kg⁻¹. In a research an electrochemical aptasensor has been introduced for diagnosis of mycotoxins (ZEN and FB1) based on rMoS₂/Au NPs nanocomposite [118]. Here, a GCE was considered as a transducer and was modified with a solution containing HAuCl₄·3H₂O and MoS₂ at room temperature in order to improve the electron transfer process (Fig. 3). Then, the surface of the modified electrode was reduced by NaCl solution via an electrochemical procedure in the potential from 1.1 to -1.1 V. The average size of Au NPs was 15–20 nm. Subsequently, solutions containing two thiol-functionalized aptamers (aptamer 1: ZEN and aptamer 2: FB1) were dropped on the surface of the electrode and established

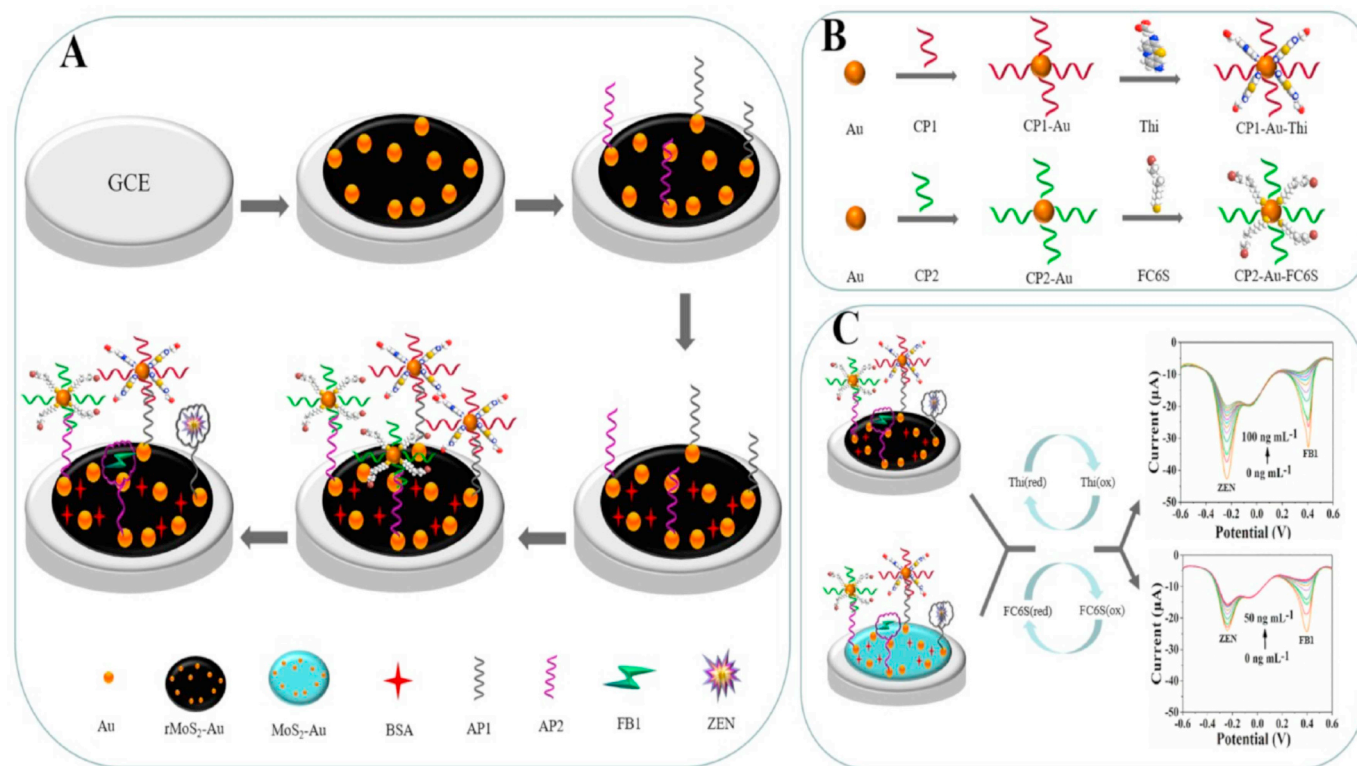


Fig. 3. Simultaneous detection of ZEN and FB1 mycotoxins using an electrochemical aptasensor equipped with rMoS₂-Au nanocomposite; License Number: 4715241100230.

the immobilization process through conjugation with Au molecules (Au-S covalent bond). On the other side, the amine-functionalized complementary DNA sequences termed as CP1 and CP2 were prepared as a conjugated form with Au NPs and signal probes. Thi and 6-(Ferrocenyl) hexanethiol (FC6S) as the signals probes were applied in the structure of CP1-Au-Thi and CP2-Au-FC6S, respectively. CP1-Au-Thi was used against aptamer-1 and could hybridize with this aptamer in the absence of ZEN as the analyte. Besides, CP2-Au-FC6S was used against aptamer-2 and could hybridize with this aptamer in the absence of FB1 as the analyte. In the presence of analytes (ZEN and FB1), due to a higher affinity between each aptamer and related analyte, the double-stranded hybridized structures were broken, and aptamer 1-ZEN and aptamer 2-FB1 created. This phenomenon was led to a decrement in conductivity and reduces the rate of electron transfer. So, the peak current decreased in the presence of various concentrations of analytes gradually. In another evaluation, the performance of the aptasensor was followed when rMoS₂-Au and MoS₂-Au applied for surface modification of the GCE. The results confirmed that rMoS₂-Au nanocomposite was more controllable and showed a higher binding activity; the use of rMoS₂-Au nanocomposite was led to substantial improvements in sensitivity and other analytical features of the designed aptasensor. This aptasensor could detect the presented mycotoxins in a linear range: 1×10^{-3} to 10 ng mL^{-1} (ZEN) and 1×10^{-3} to $1 \times 10^2 \text{ ng mL}^{-1}$ (FB1) while the LOD for both was reported equal to $5 \times 10^{-4} \text{ ng mL}^{-1}$.

Microcystin (C₄₉H₇₄N₁₀O₁₂) is a cyclic heptapeptide and recognized as the most abundant cyanotoxin produced worldwide; this toxin is the most common hepatotoxin produced by blue-green algae (cyanobacteria) [119]. Microcystin is the most important threatening factor for drinking water and, in high doses, causes hepatic hemorrhage and death in a short period of time. It should be noted that the maximum allowed concentration of this toxin in drinking water is $1 \mu\text{g L}^{-1}$. In a research, Microcystin-Leucine-Arginine (MC-LR) as a toxin was diagnosed by an electrochemical aptasensor [120]. Here, a three-

dimensional nanocomposite (AuNPs@MoS₂)/TiO₂ nanobeads (TiONBs) was synthesized from a mixture and could modify the surface of a GCE as the transducer. In order to find finally achieved three-dimensional nanocomposite, initially, MoS₂-TiONB nanocomposite was synthesized from TiONBs, Na₂MoO₄·2H₂O, and C₂H₅NS; then, HAuCl₄·3H₂O was added, and AuNP@MoS₂-TiONB obtained. Then, a thiol-functionalized aptamer was immobilized on the surface of the modified electrode with AuNP@MoS₂-TiONB and an Au-S covalent bond created between the 5' end of aptamer and AuNPs. In the next step, a mixture containing a biotin-functionalized complementary DNA strand and various concentrations of analyte was prepared and dropped on the surface of the GCE. Finally, the avidin conjugated horseradish peroxidase (avidin-HRP) was added and bound to complementary DNA; at this time, the designing steps of this aptasensor finished. The aptasensing mechanism was based on an enzymatic reaction (oxidization of hydroquinone (HQ) to benzoquinone (BQ)) catalyzed by HRP. In the presence of the analyte, the aptamer captured it, and most of hybridized double-stranded DNA (aptamer-complementary DNA) structures were broken; this event was led to reducing the amount of avidin-HRP. So, the reduction of BQ decreased along with the increment concentration of MC-LR. This relation provided a quantitative method for the determination of this toxin. The obtained linear detection range by this aptasensor was 0.005–30 nM, with a LOD about 0.002 nM. Arsenic is a carcinogenic metalloid element that widespread presence of it in unauthorized quantities in nature has involved many countries at risk. Arsenic toxicity is a function of its constituents [121]. In terms of composition, organic and inorganic arsenic are considered as two categories. The most crucial arsenic compounds in aquatic environments are mono-methyl arsenic, arsenite (As(III)), pentavalent arsenate (As(V)), and dimethyl arsenic, respectively. Among the arsenic oxidized types, As(III) and As(V) are the most common oxidative types in nature, which As(III) is more toxic than As(V). As(III), as heavy toxic metal, was diagnosed by an electrochemical aptasensor based on 3D-rGO modified AuNPs [122]. In this research, a GCE was applied as the working

electrode and modified with a nanocomposite (3D-rGO/AuNPs). This nanocomposite was synthesized from oxidized graphite, HAuCl₄, and glucose. Similar to the other investigated researches in this review, the role of applied nanostructures was enhancing the active surface area for interaction with the biorecognition element, which can be on the transducer or in a conjugation form in other sensing elements and far from the transducer. Then, a thiolated aptamer was immobilized on the surface of the modified GCE with 3D-rGO/AuNPs, and a strong covalent bond (Au-S) created between the thiol group of aptamer and AuNPs. In the presence of As(III), the conformation of the aptamer changed and could capture the analyte with high affinity. When the analyte was captured with the aptasensor, the Rct value increased along with the concentration. The obtained differences between the output EIS signals related to each concentration of As(III) provided an electrochemical method for the exact determination of this material. This aptasensor could determine the analyte in a linear range from 3.8×10^{-7} to 3×10^{-4} ng mL⁻¹, and the obtained LOD was about 1.4×10^{-7} ng mL⁻¹. Bisphenol A is an organic compound and contains two phenolic groups. This material is an essential component of several polymers and polymer additives. Bisphenol A has been widely used in many products worldwide; this means that everyone is partially confronted with it. This exposure can be through the consumption of food and drinks, where this material is used in packaging and constant contact with it. Bisphenol A can cause many complications [123], including genetic disorders, decreased sperm count and testosterone levels, ovarian cysts, breast and prostate cancer, liver disorders, and brain damage, such as learning and memory disorders. In a research, bisphenol A was detected by an electrochemical aptasensing approach facilitated by MWCNT-SiO₂@Au nanocomposite [124]. In order to synthesize the nanocomposite, several steps were followed; initially, colloidal spheres silica NPs were obtained from tetraethylorthosilicate and then functionalized with the amino group of 3-aminopropyltriethoxysilane; on the other side, colloidal Au NPs were synthesized from HAuCl₄ and attached to silica NPs via dispersing in ethanol. Afterward, a shell of Au NPs was grown on the silica/aminopropyltriethoxysilane/Au NPs (core). Finally, MWCNT was attached to SiO₂@Au nanocomposite through sonication in a mixture containing dimethylformamide. Here, a GCE was applied as the working electrode in a three-electrode system and modified with MWCNT-SiO₂@Au nanocomposite. The aptasensor was ready to use after immobilization of a thiolated aptamer (biorecognition element) on the surface of the electrode. The mechanism of detection was based on access to the redox marker (ferro/ferricyanide) molecules; in the absence of the analyte, the accessible free spaces for redox marker molecules were at a high level and resulted in creating a robust output electrochemical signal. Nonetheless, in the presence of the analyte, most of the aptamer strands could capture analyte molecules, and accessible free spaces for ferro/ferricyanide molecules were reduced extremely. This event was led to reducing the electron transfer rate between the electrolyte and transducer, where the peak current of output electrochemical signals reduced along with the increment of analyte concentration. This signal-off aptasensor could detect the mentioned organic compound in a linear range from 0.1 to 100 nM with a LOD equal to 10 pM. Lead is the fourth most widely used element in the world. It has a metallic sheen, low conductivity, and has a high malleable property. Besides, this metal is highly corrosion resistant. Lead is extremely toxic and can cause physiological, biochemical, and behavioral disorders in humans and animals [125]. Based on the WHO criteria, the maximum concentration of lead ion (Pb²⁺) in drinking water should not be more than 48 nM. In a research, Pb²⁺ was determined by an electrochemical aptasensor integrated with Au modified porous rGO (Au@p-rGO) and Au@GO nanocomposites [126]. In this study, a GCE was applied as the transducer and modified with Au@p-rGO nanocomposite; Then, a thiolated aptamer (aptamer-1: 32-mer) was immobilized on the surface of the electrode. On the other side, Au@GO nanocomposite was synthesized and conjugated with a thiol-amine-functionalized aptamer (aptamer-2:

39-mer); afterward, Au@GO/aptamer-2 was immobilized on the surface of the electrode through the hybridization between aptamer-1 and aptamer-2 (Fig. 4). Finally, the prepared aptasensor was used for diagnosing various concentrations of Pb²⁺. The electrolyte solution was containing ferro/ferricyanide as the redox marker and hydrogen peroxide (H₂O₂). The detection of analyte was based on the catalytic reaction of added H₂O₂ and Au@GO/aptamer-2. The Pb²⁺-dependent DNazymes strategy was applied in the presence of the analyte, and H₂O₂ converted to H₂O. The differences between electrochemical signals in the presence and absence of the analyte were led to determining the analyte. This signal-off aptasensor was able to detect Pb²⁺ in a dynamic range from 5 pM to 1 μM, while the LOD was 1.67 pM.

Mercury is one of the heavy metals found in the earth's crust. It enters the environment through natural phenomena such as the eruption of volcanoes. Currently, human activities such as burning coal and extracting Au are major contributors to the release of mercury into nature. Mercury is more volatile than all metals, and its vapor is very toxic [127]. Mercury penetrates the bloodstream from the lungs, then passes through the blood-brain barrier (BBB) and, by entering the brain, causes severe damage to the central nervous system. Genetic disorders, weakening of the cardiovascular system, hypertension, kidney, and gastrointestinal problems are other potential challenges for mercury exposure. In a research, an electrochemical aptasensor was developed for the diagnosis of mercury ion (Hg²⁺) [128]. Initially, a GCE was considered as the working electrode and modified with the Au modified thiol reduced graphene (Au@HS-rGO) nanocomposite as an electron transfer facilitator. The modification process was performed through physical adsorption. Then, a thiol-functionalized aptamer was immobilized via the Au-S bond on the surface of the electrode as the biorecognition element. It should be considered that the thymine base of the aptamer strand can bind to Hg²⁺ through stable thymine-Hg²⁺-thymine interactions. So, in the presence of Hg²⁺, due to a high affinity between the aptamer and analyte, the aptamer conformation's changes and folding occurred. Subsequently, Thi as a signal marker was embedded in the folded aptamer strands; so, determining the electrochemical signal of embedded Thi in the folded aptamer strands showed a parallel association against the concentrations of Hg²⁺. The mentioned signal-on aptasensor could determine the analyte in a linear range from 1 to 200 nM, and the reported LOD was equal to 0.38 nM. In Table 2, significant aspects of recent electrochemical aptasensors based on the Au nanostructures for the diagnosis of toxins, metal ions, and chemical compounds have been provided.

4. Electrochemical aptasensors based on the Au nanostructures for diagnosis of biomarkers

Biomarkers are biological molecules and, based on their properties, can be present in blood, feces, urine, tissues, or other body fluids. Different types of molecules, such as DNA, genes, proteins, hormones, and cells, can act as biomarkers. Biomarkers indicate the physiological or pathological condition of a particular organ. Pathologic biomarkers are used in the screen, diagnosis, prognosis, and assessing response to therapy of various diseases [154]. Thrombin is a protein that plays a crucial role in blood coagulation, clot dissolution, and tissue repair. Thrombin can also act as a regulator of platelet aggregation, endothelial cell activation, and other essential responses in the vascular system [155]. In a research, a PEC aptasensor has been introduced for the determination of various concentrations of thrombin [156]. Here, a GCE was considered as the transducer, and a layer of Au NPs was electrodeposited on the surface of it at -0.2 V for 30 s (Fig. 5). Afterward, the prepared electrode was modified with perylene tetracarboxylic acid (PTCA) as a PEC organic dye; subsequently, another layer of Au NPs was electrodeposited on the surface of the transducer it at -0.2 V for 15 s. Then, an amine-functionalized thrombin aptamer was immobilized on the surface and could provide an amine-Au bond with the Au NPs. So, a structure containing GCE/Au NPs/PTCA/Au

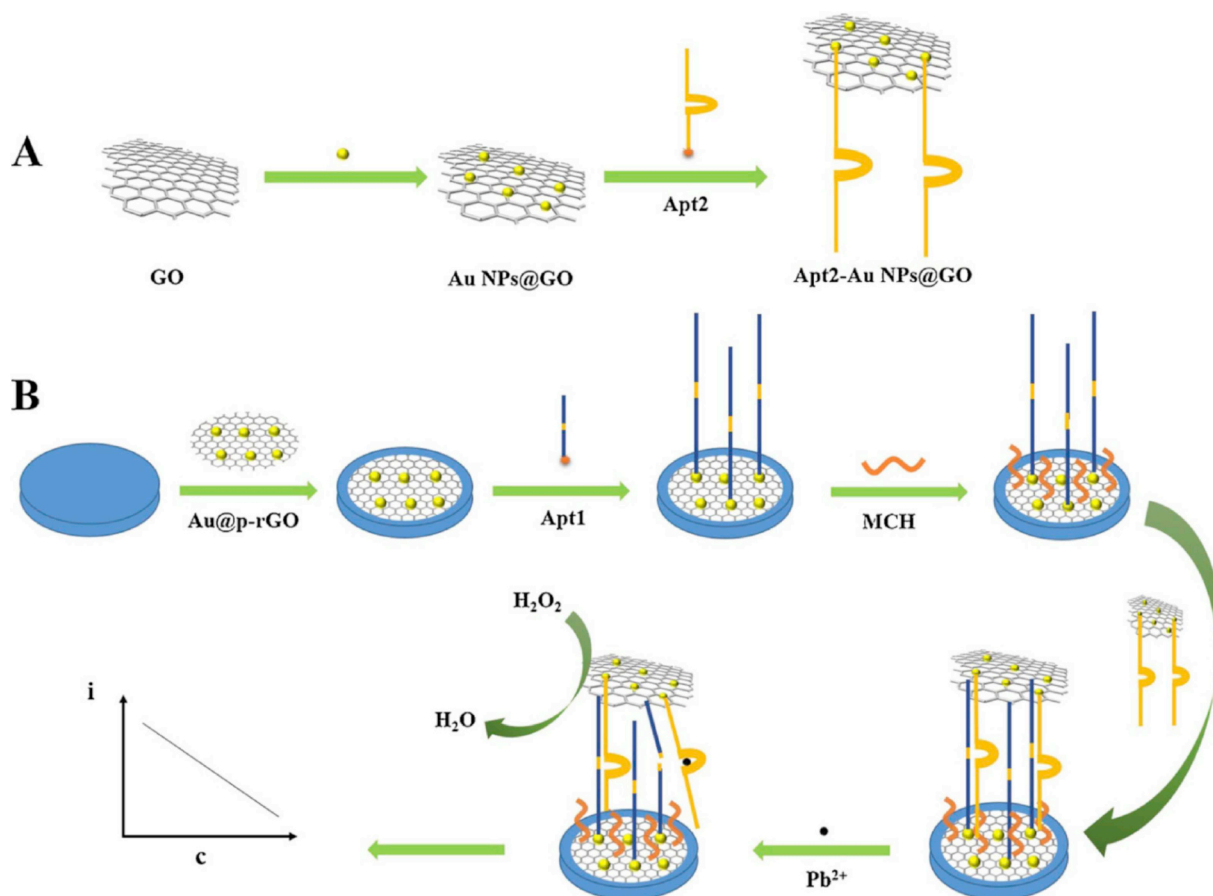


Fig. 4. The detail of electrochemical aptasensor for diagnosis of Pb^{2+} ; License Number: 4797701411741.

NPs/aptamer was obtained. Then, the electrode was immersed in a concentration of thrombin and this analyte captured by the aptamer immobilized on the surface from one side; at the next step, another amine-functionalized thrombin aptamer was added on the surface of the transducer and could capture the analyte from other side and produce a sandwich structure form. Then, glutaraldehyde was added; finally, $C_3N_4@C60$ core-shell nanocomposite as quencher was added on the surface, and the PEC output signal of prepared aptasensor was measured for various concentrations of analyte (Fig. 5). The competition between C_3N_4 and PTCA for light absorption in the presence of electron donor ascorbic acid (AA), provided a different photocurrent when the sandwich structure form existed or in the absence of thrombin. This signal-off PEC aptasensor was able to diagnosis the mentioned biomarker in a linear range from 10 fM to 10 nM with a LOD equal to 1.5 fM.

In a research, human liver hepatocellular carcinoma cells (HepG2) as a cell line of liver cancer were detected by an electrochemical aptasensing platform [157]. In the first step, an Au electrode was considered as the working electrode, and then a structure containing HepG2 aptamer, and a DNA tetrahedron sequence was immobilized on the surface of it. DNA tetrahedron was produced from three thiol-functionalized DNA strands for immobilization (Au-S bond) on the surface of the Au electrode and one linking aptamer strand for hybridization with HepG2 aptamer. The reason for the use of a DNA tetrahedron sequence was improving the specificity and capture efficiency of this aptasensor. Afterward, a typical concentration of HepG2 cells was dropped on the surface of the working electrode and captured by the aptamer. Finally, the functional hybrid nanoprobe (prepared from MIL-101(Fe) as a MOF, AuNPs (MIL-101(Fe)@AuNPs), DNzyme, hemin, and HRP) was dropped on the surface of working electrode and established a sandwich-like structure; then, the electrochemical

behavior of the prepared aptasensor was followed in the presence of a solution containing HQ and H_2O_2 . In the presence of the analyte, HQ oxidized to BQ via an enzymatic reaction catalyzed by HRP; at this time, in another reaction, H_2O_2 was converted to H_2O . The changes in the output electrochemical signals were led to the quantitative detection of HepG2 cells. This signal-on aptasensor could detect this cancer biomarker in a linear range from 0 to 1×10^7 cells mL^{-1} , while the calculated LOD was 5 cells mL^{-1} . Breast cancer is the most common and most crucial malignancy among women worldwide. Over-expression of the ERBB2 gene is commonly reported in patients with breast cancer. Human epidermal growth factor receptor 2 (HER2) is a protein encoded by the mentioned gene. In recent years, this protein has become one of the most important diagnostic and prognostic biomarkers in breast cancer patients [158]. Tumor necrosis factor α (TNF- α) is one of the essential proteins in the signaling pathway and plays a critical role in systemic inflammation, the acute phase response, and inhibition of tumor progression [159]. The TNF- α molecule is produced by a variety of hematopoietic and non-hematopoietic and malignant cells. These cells include macrophages, B lymphocytes, T lymphocytes, natural killer (NK) cells, neutrophils, astrocytes, endothelial cells, smooth muscle cells, and more. In a research, an electrochemical aptasensor was designed for the detection of TNF- α based on a graphite screen-printed electrode as the transducer [160]. At the first step, the graphite screen-printed electrode was modified with cobalt hexacyanoferrate (CoHCF) by an electrochemical procedure, and then the electrode was physically modified with the colloidal Au NPs. Afterward, a thiolated aptamer was immobilized on the surface of the modified electrode with CoHCF/Au NPs. The strands of aptamer were attached to the surface of Au NPs through the Au-S bond. Subsequently, a typical concentration of TNF- α was dropped on the surface of the modified electrode; at this time, TNF- α was captured by the aptamer strands from

Table 2

Type of analyte	Aptamer sequence	Type of Au nanostructure	Detection technique	Detection range	LOD	Ref.
Aflatoxin B ₁	5'-NH ₂ -(CH ₂) ₆ -GTTGGGCAGGTGTGTCTCTCTCTGTCTCTCGTTCGCCCTCCG TAGGCCACACA-3'	Au NPs	PEC	0.03–200 ng mL ⁻¹	0.01 ng mL ⁻¹	[47]
Aflatoxin B ₁	5'-GTTGGGCACGTGTGTCTCTCTCTGTCTCTCGTGCCCTTCGCTAGGCCACACA-Fc-3'	Au NPs	DPV/EIS	0.1 pg mL ⁻¹ - 10 ng mL ⁻¹	0.049 pg mL ⁻¹	[51]
Aflatoxin B ₁	5'-GTTGGGCACGTGTGTGTCTCTCTCTCTGTCTCTGTGTGCCCCTCGTAGGCCCA-3'	Cu-MOF/Au NPs nanocomposite	DPV	10 ⁻⁶ - 1 ng mL ⁻¹	6.7 × 10 ⁻⁷ ng mL ⁻¹	[48]
Aflatoxin B ₁	5'-TGGGGTTTTGTGTGCGC GTGGTCTACGGCGCAGGG-3'	Au NR	DPV	1 pM - 0.25 nM	0.3 pM	[129]
Aflatoxin B ₁	5'-GTTGGGCACGTGTGTGTCTCTCTCTGTGTCTCTGTGCCCCITTCGCTAGGCCACACA-3'	Au NPs/SiO ₂ @Fe ₃ O ₄ ; MoS ₂ /Au NPs nanocomposites	DPV	0.1 fg mL ⁻¹ -0.1 µg mL ⁻¹	0.01 fg mL ⁻¹	[46]
Aflatoxin M ₁	5'-TTATGTCTCTCTCTGTGTGCGCATTTCTCTCTCTGTGTGCGCATTTGGAAGTTGGTAAG GAGGAGACATAATTACCAA-(CH ₂) ₆ -SH-3'	Au NPs	ECL	0.4 pg mL ⁻¹ - 400 ng mL ⁻¹	0.09 pg mL ⁻¹	[22]
Aflatoxin M ₁	5'-TAAACACGACACTGTCTAGATTTTCCACATTTCTCTGTTC-C-SH-3'	Au NPs	DPV	2–600 ng L ⁻¹	0.9 ng L ⁻¹	[43]
Ochratoxin A	5'-SH-GATCGGGTGTGGTGGCGGTAAAGGGAGCATCGGACA-3'	Poly (3,4-ethylenedioxy thiophene) (PEDOT)/Au NFs nanocomposite	CV	0.01–20 ng L ⁻¹	4.9 pg L ⁻¹	[50]
Ochratoxin A	5'-TTTTTGATCGGGTGTGGTGGCGGTAAAGGGAGCATCGGACA-3'	Au NPs	EIS	50 fg mL ⁻¹ - 10 ng mL ⁻¹	5.2 fg mL ⁻¹	[130]
Ochratoxin A	5'-GATCGGGTGTGGTGGCGGTAAAGGGAGCATCGGACA-3'	Au NPs	DPV	0.001–500 parts per billion (ppb)	0.001 ppb	[42]
Staphylococcal Enterotoxin B	5'-TGCAGGATCCGGTATCCGTGCACACACACCACACACGCTGCCGACCGGAGG AATTTCGT-3'	Au nano-urchins (Au NUs)	DPV	5 - 500 fM	0.21 fM	[44]
Patulin	5'-CCCGCGCGCGCAACCCGCGATCATCTACACTGATATTTTACCTTCC-SH-3'	Black phosphorus (BP)/Au NPs nanocomposite	EIS	0.1 nM - 10 µM	0.03 nM	[131]
Malathion	5'-COOH-ATCCGTACACACCTGCTCTTATACAAAT TGTTTTCTCTTAACCTTGACGTGCTGTGTGGGT-3'	Au NPs	DPV	0.5–600 ng L ⁻¹	0.5 ng L ⁻¹	[132]
Carbendazim	5'-C ₆ -SH-GGGCACACAAACGATGGTCCAGCCACCCGAATGACC AGCCACCCGCCCAACCCGCG-3'	Carbon nanohorns/Au NPs nanocomposite	EIS	1–1000 pg mL ⁻¹	0.5 pg mL ⁻¹	[133]
Bisphenol A	5'-SH-(CH ₂) ₆ - CCGTGGGTGTCAGGTGGGATAGGGTTCCGGTATGGCCAGCGCATCAGGGTTCGCA CCA-3'	Au NPs	EIS	0.5 fM - 5 pM	80 aM	[134]
Bisphenol A	5'-SH-(CH ₂) ₆ -CCGGTGGGTGTCAGGTGGGATAGCGTTCGGCGTATGGCCAGCGC ATCACGGGTTCGGACCA-3'	Au NPs	CV/DPV	0.01–120 µM	0.53 nM	[135]
Bisphenol A	5'-SH-(CH ₂) ₆ -CCGGTGGGTGTCAGGTGGGATAGCGTTCGGCGTATGGCCAGCGCAT CACGGGTTCGCAACA-3'	MWCNT-SiO ₂ @Au core-shell nanocomposite	DPV	0.1–100 nM	10 pM	[124]
Bisphenol A	5'-SH-(CH ₂) ₆ -CCGGTGGGTGTCAGGTGGGATAGCGTTCGGCGTATGGCCAGCGCAT CACGGTTCGCAACA-3'	MWCNT/Fe ₃ O ₄ @Au nanocomposite	DPV	0.1–8 nM	0.03 nM	[136]
Bisphenol A	5'-SH-(CH ₂) ₆ -CCGGTGGGTGTCAGGTGGGATAGCGTTCGGCGTATGGCCAGCGCA TCAGGGTTCGCA CCA-3'	Au/CuFe ₂ O ₄ -Pr-SH/MW CNTs nanocomposite	DPV	0.05–9 nM	25.2 pM	[137]
Acetaminprid	5'-SH-(CH ₂) ₆ -TGTAAATTTGTCGACGGGTCTTTGATCGCTGACACCA TATTATGAAGA-3'	Graphene quantum dot/Au nanostars nanocomposite	DPV	0.001 - 1000 pM	0.0003 pM	[138]
ZEN	5'-TCATCTATCTATGTTACATTACTATCTGTAATGTGATATG-(CH ₂) ₆ -SH-3'	Pt@Au nanocomposite	CV	0.5 pg mL ⁻¹ - 50 ng mL ⁻¹	0.17 pg mL ⁻¹	[139]
ZEN	5'. SH-AGCACACAGAGTCAGATGTCAICTATCTATGTGTACATTACTATCTGT AAATGTGATGOCATATGGTGCTACCGTGAA-3'	Au NPs	DPV	20–80,000 ng L ⁻¹	10 ng L ⁻¹	[140]
ZEN	5'-TCATCTATCTATGTTACATTACTATCTGTAATGTGATATG-3'	Hollow cubic platinum@Au nanoframes functionalized polyethyleneimine- (hcPt@Au NFs/PdI+GO) nanocomposite	DPV	0.5 pg mL ⁻¹ - 50 ng mL ⁻¹	0.105 pg mL ⁻¹	[141]
ZEN	5'-SH-(CH ₂) ₆ -AGCAGCACAGAGGTGCAGATGTCTATCTATCTATGTGTAATTACTATCTGT AAATGTGATGOCATATGGTGCTACCGTGAA-3'	porous platinum nanotubes (pNNTs)/Au NPs/Thi/GO nanocomposite	DPV	0.5 µg mL ⁻¹	0.17 pg mL ⁻¹	[142]
ZEN/FBI	Apt1: 5'-SH-(CH ₂) ₆ -TCATCTATCTATGTFACATTACTATCTGTAAATGTGATATG-3' Apt2: 5'-SH-(CH ₂) ₆ - ATACAGCTTATTCAATTAATCGCATTAACCTTATACCAAGCTTATTCAAATTACGTTCTGCACATACCA GCCTTATTCATATGATAGTAAGTGAATCT-3'	MoS ₂ /Au NPs nanocomposite	DPV	0.5 pg mL ⁻¹ - ZEN: 1 × 10 ⁻³ , FBI: 1 × 10 ⁻³ - 1 × 10 ⁻² ng mL ⁻¹	5 × 10 ⁻⁴ ng mL ⁻¹	[118]

(continued on next page)

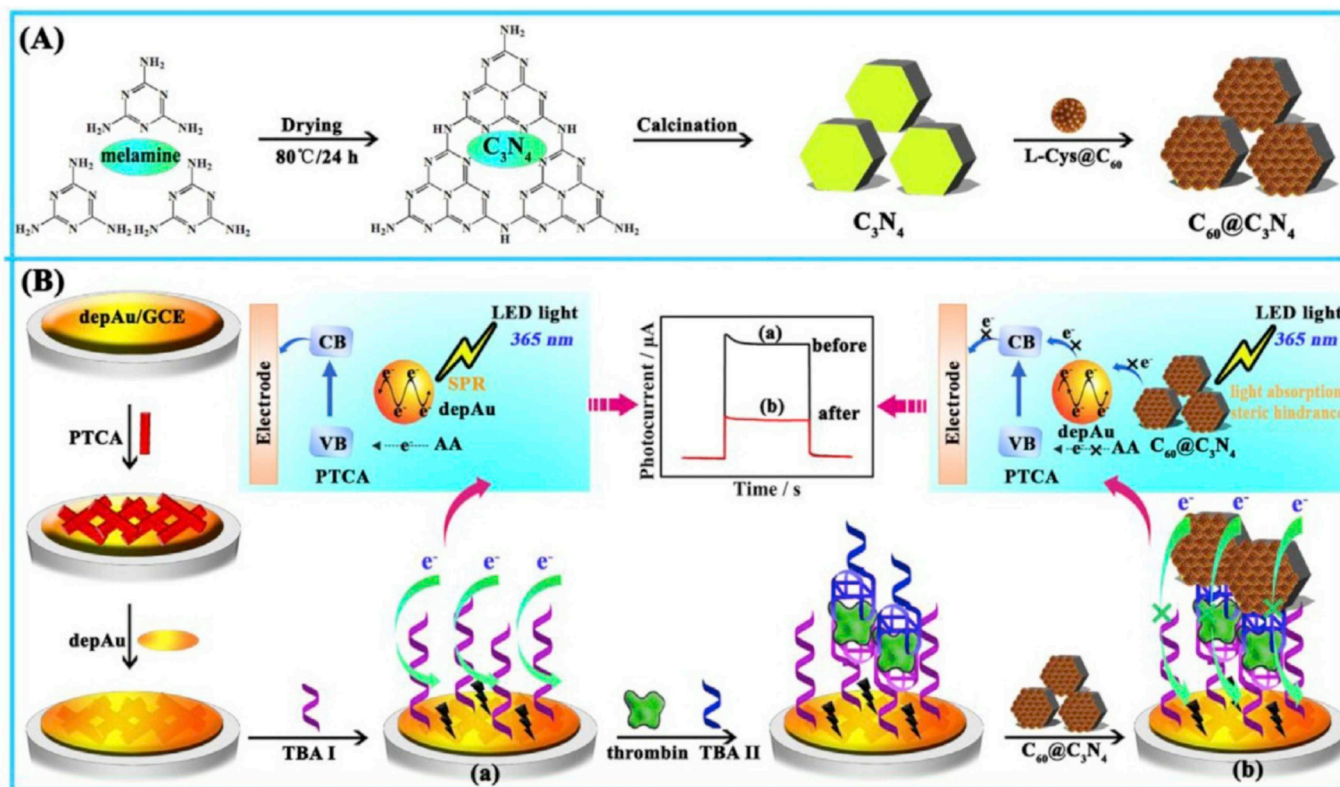


Fig. 5. Various designing steps of a PEC aptasensor for diagnosis of thrombin; License Number: 4715221343598.

one side. Finally, a mixture containing a conjugated antibody-HRP was dropped on the surface of the electrode, and the applied antibody could capture TNF- α from the other side; this aptamer-antibody sandwich assay platform applied for the quantitative determination of TNF- α . The establishment sandwich structure was led to reducing the rate of electron transfer and increment of Rct. The differences between the output electrochemical signals before/after the formation sandwich structure provided an analytical tool for the detection of this biomarker. The found linear detection range of the mentioned aptasensor was from 1 to 100 pg mL⁻¹, and the LOD was about 0.52 pg mL⁻¹. Vascular endothelial growth factor (VEGF) is one of the cytokines and the most critical angiogenic regulator (useful in the growth and development of new vessels). The association between increased expression of this growth factor and tumor progression has been reported in several cancers [161]. On the other side, MCF-7 cells are considered as a breast cancer cell line that isolated in 1970 from a woman. The carcinoembryonic antigen (CEA) is a glycoprotein that naturally produced in the fetal digestive tissue (cut-off value: 5 ng mL⁻¹). After birth, its serum level is very low and cannot be measured in healthy adults. This biomarker is used to diagnose or determine the severity and prognosis of cancer patients (especially breast cancer, colorectal carcinoma, cervical carcinoma, and ovarian cancers) and also used to control and treat several cancers [162]. Interleukins are a large family of cytokines that most cells can synthesize them. These cytokines increase their biological response by binding to specific receptors on the surface of target cells. Several interleukins, especially those that can regulate the growth of the deformed cells, have been implicated in the diagnosis and treatment of diseases, especially some types of cancers [163]. Lower than normal values of dopamine can lead to Alzheimer's disease, Parkinson's disease, attention-deficit/hyperactivity disorder (ADHD), Huntington's disease, schizophrenia, and some other diseases. These diseases are caused by a disorder in the neurons involved in the production of dopamine. A deliberate increase of dopamine levels is also caused by people abusing drugs; this increment is intended to induce

joy, excitement, and pleasant emotions. The normal concentration of dopamine should be between 10 and 1000 nM. Fast and accurate detection of this neurotransmitter can show its physiological function in the body and will be applicable to prevent and treatment of the mentioned diseases in some cases [164]. In a research, the spindle-shaped Au nanostructure was synthesized and applied in the structure of an electrochemical aptasensor for the diagnosis of dopamine [10]. Initially, an Au electrode was considered as the working electrode in a three-electrode system and then modified with the spindle-shaped Au nanostructure (80–200 nm). The nanostructure synthesizes solution was a mixture of H₂SO₄, HAuCl₄, and sodium dodecyl sulfate (SDS). The modification surface of the Au electrode with the nanostructure was performed via an electrodeposition procedure at -0.3 V for 5 min. Then, a thiol-functionalized aptamer was applied as the biorecognition element and immobilized on the surface of the working electrode via the Au-S bond. In the absence of analyte, due to the negative charge of free aptamers, the peak current of aptasensor was in minimum; in the presence of dopamine, due to a high affinity between the biorecognition element and analyte, the conformation of aptamers changed, and the most of strands could capture the molecules of the analyte. So, the free strands of aptamer were reduced along with the increment concentration of the analyte. This event was led to reduce the net negative charge of aptamer and increment the peak current of aptasensor against various concentrations of dopamine. The linear detection range of this signal-on aptasensor was from 25 pg mL⁻¹ to 3 ng mL⁻¹, while the obtained LOD was about 2 pg mL⁻¹. Alzheimer's disease is a progressive neurodegenerative disease that reduces thinking and leads to behavioral changes in individuals. It is the most common form of dementia. One of the pathologic causes of this disease is the accumulation of amyloid-beta (A β) peptides around the brain cells and neurofilaments within the neurons [165]. These amyloid plaque accumulations will act as inhibiting neural function and impairing memory. Recent studies also show that A β produced elsewhere in the body can reach the brain and lead to Alzheimer's-like symptoms. In a research, an

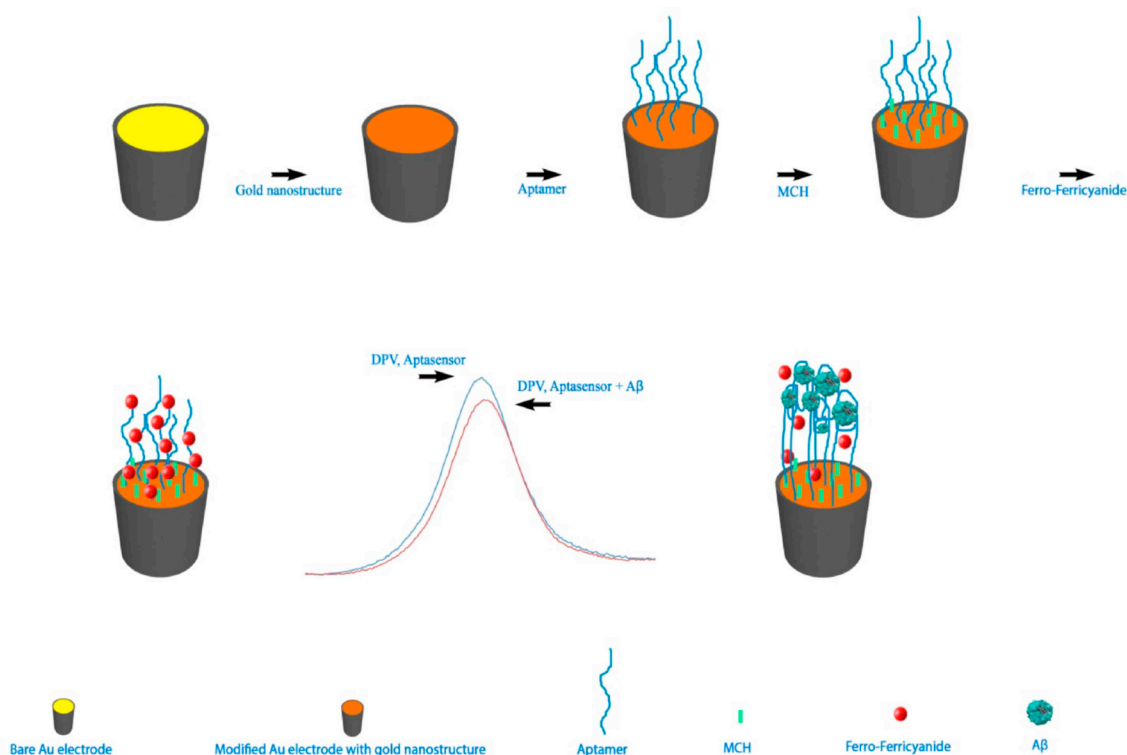


Fig. 6. Various steps for designing Alzheimer's disease aptasensor; License Number: 4797710511798.

electrochemical aptasensing platform has been introduced for early diagnosis of A β as the primary biomarker of Alzheimer's disease [8]. Here, the transducer was a modified Au electrode with a fern leaves-like Au nanostructure. This nanostructure was produced from H₂SO₄, HAuCl₄, and polyethylene glycol (PEG) 6000. This synthesized nanostructure on the surface of the Au electrode provided a large and optimized surface area for immobilization of the biorecognition element (a thiolated aptamer (107-mer)). The aptamer was immobilized on the enhanced surface area of the modified Au electrode with nanostructure and established a covalent Au–S bond (Fig. 6). The presence of the analyte was a reducing conductivity of transducer, and the weakening rate of electron transfer was led to the reduction of peak current dramatically. This signal-off aptasensor was able to detect A β in a dynamic range from 0.002 to 1.28 ng mL⁻¹, and the obtained LOD was about 0.4 pg mL⁻¹.

Tau is one of the major proteins present in axons that stabilize the microtubules forming the neural pathways and the neurotransmission [166]. The hyperphosphorylated form of tau is insoluble, in which case its tendency to bind to microtubules is reduced and spontaneously forms neurofibrillary tangles. Increased levels of phosphorylated tau in cerebrospinal fluid can be a useful biomarker in predicting and diagnosing the early stages of Alzheimer's disease. In a research, Tau381 was detected by an electrochemical aptasensing platform [167]. Initially, a GCE was considered as the working electrode and modified with carboxyl graphene, thionin, and Au NPs, respectively. Thionin, as a phenothiazine cationic dye (signal probe), could provide a link between graphene and Au NPs. Afterward, an amine-functionalized aptamer was immobilized on the surface of the working electrode through Au-amine and hydrogen bonds. Finally, the aptasensor was used for determining the various concentrations of the analyte. The electrochemical redox behavior of thionin in the absence/presence of Tau381 provided a quantitative tool for the diagnosis of this biomarker. The proposed signal-on aptasensor was able to the diagnosis of Tau381 as a biomarker of Alzheimer's disease in a dynamic range from 1 to 100 pM while the obtained LOD was about 0.7 pM. The details of aptasensors

based on the Au nanostructures designed to diagnosis different biomarkers cited in Table 3. It should be noted that a number of aptasensors designed to detect different cancer biomarkers as well as biomarkers associated with myocardial infarction and those applications have recently been reviewed in another study [65].

5. Electrochemical aptasensors based on the Au nanostructures for diagnosis of pathogen microorganisms

Microorganisms are included protozoa, algae, fungi, bacteria, and viruses [182]. A number of these microorganisms are the leading infectious agents and lead to diseases such as tuberculosis, influenza, etc. Quicker diagnosis can be beneficial in earlier treatment and prevention of outbreaks. On the other hand, a specific diagnosis can play a very significant role in targeting drug delivery, reducing costs, and adopting specific treatment. In a research, an electrochemical aptasensor has been introduced that was able to detect LPS from *Escherichia coli* 055:B5 [40]. LPS is considered as the main element of the membrane in the gram-negative bacteria. LPS as a dangerous and deadly endotoxin is led to septic shock in hospitalized patients. So, evaluating and determining the value of this toxin is unavoidable. Here, a GCE was modified with rGO/Au NPs nanocomposite, and an amine-functionalized aptamer applied for LPS determination. At the first step, rGO/Au NPs nanocomposite was incubated and mixed with the aptamer through EDC and NHS (0.5 mg mL⁻¹). Then, rGO/Au NPs/aptamer was dropped on the surface of GCE and dried at room temperature. The prepared aptasensor was applied for LPS detection in the presence of [Fe (CN)₆]^{-3/-4} as the redox marker. Designed aptasensor was signal-off, and in the presence of the analyte, the Rct increased along with the concentrations of LPS. This aptasensor could detect LPS in a linear range from 0.1 to 0.9 pg mL⁻¹, and the LOD was calculated as 1 fg mL⁻¹. In another research, an aptasensor has been developed to quantitative analysis of the corrosion induced by sulfate-reducing bacteria (SRB) [183]. Unfortunately, microbiologically induced corrosion (MIC) is occurred principally by SRB (about 50% of total corrosion). This challenge has

Table 3
Main features of electrochemical aptasensors based on the Au nanostructures for diagnosis of biomarkers.

Type of biomarker	Aptamer sequence	Type of Au nanostructure	Detection technique	Detection range	LOD	Ref.
BCM-7	5'-NH ₂ -ATACGGGAGCCACACACCAAGTAAGATCATCACCCGGACGGGACATAATAGGAG AGCAGGTGTGACGGAT-3'	Au NR	DPV	1 fM - 25 nM	334 aM	[34]
HepG2 cells	5'-SH-(CH ₂) ₆ -ACAGCATCCCATCTGTGAACAATCGCATTTGTGATTGTTAGGTTTCCCGC CTCATGGACGGTGTG-3'	Au NPs	DPV	50–1 × 10 ⁶ cells mL ⁻¹	15 cells mL ⁻¹	[168]
HepG2 cells	5'-ACAGCATCCCATCTGTGAACAATCGCATTTGTGATTGTTAGGTTTCCCGCCTCATGG ACGTGCTG-3'	Au NPs	DPV	0–1 × 10 ⁷ cells mL ⁻¹	5 cells mL ⁻¹	[157]
Aβ	5'-SH-TTTTTTTTTTTGGAAUUCGAGCUGCUACCUUUAACCGUAAAGCCUGUCUUC GUUUCACAGCGCUUGUAGCCUCACACUUUGUA CCUGGCGCAACUGCAGCAUGCAAGCUUGG-3'	Fern leaves-like Au nanostructure	DPV	0.002–1.28 ng mL ⁻¹	0.4 pg mL ⁻¹	[8]
Aβ	5'-SH-GCCTGTGTGTGGGCGGGTGG-3'	Au NFs/Au NPs	DPV	1 nM - 2 mM	0.45 nM	[169]
CEA	5'-ATACAGCACTTAATCAATT-3'	ZnO flower-rod/g-C ₃ N ₄ /Au NPs nanocomposite	PEC	0.01–2.5 ng mL ⁻¹	1.9 pg mL ⁻¹	[170]
CEA	Apt 1: 5'-SH-(CH ₂) ₆ -ATACAGCTTATTCAAATT-3' Apt 2: 5'-SH-(CH ₂) ₆ -CCCATAGGAAAGTGG GGA-3'	Patchy Au coated Fe ₃ O ₄ hybrid nanoparticles (PG-Fe ₃ O ₄ NPs)	ECL	0.1 pg mL ⁻¹ - 15 ng mL ⁻¹	0.03 pg mL ⁻¹	[171]
CEA	5'-NH ₂ -(A) ₅ -ATACCAGCTTATTCAAATT-3'	Au@self-polymerized dopamine (PDA) nanocomposite	DPV	1 fg mL ⁻¹ - 1 μg mL ⁻¹	0.33 fg mL ⁻¹	[172]
HER2	5'-AAAGTAAAGAACTGATCAGCACGGGATGGGATAGGAGGGAGTGTGAAAA-3'	@Fe-MOF	DPV	10–150 ng mL ⁻¹	4.9 ng mL ⁻¹	[37]
Thrombin	Apt 1: 5'-NH ₂ -(CH ₂) ₆ -GGTTGGTGTGG-3'	Au nanospheres	PEC	10 fM - 10 nM	1.5 fM	[156]
Thrombin	Apt 2: 5'-NH ₂ -(CH ₂) ₆ -AGTCGGTGGTAGGGC AGGTGGGGCT-3' 5'-NH ₂ -(CH ₂) ₆ TTTTTTTTTTTGGTGGTGTGGTGG-3'	Au NPs	PEC	1.0 × 10 ⁻⁶ - 1.0 × 10 ⁻¹⁴ M	3.3 fM	[173]
Thrombin	Apt 1: 5'-SH-(CH ₂) ₆ -GGTTGGTGTGGTGG-3'	Au NFs	ECL	0.5–40 nM	0.08 nM	[174]
Thrombin	Apt 2: 5'-SH-(CH ₂) ₆ -AGTCGGTGGTAGGGAGGTGGGGTGACT-3'	β-cyclodextrin/Au NPs/nanographene nanocomposite	ECL	0.4–1000 pM	0.23 pM	[175]
Thrombin	Apt 1: 5'-Fc-GGTTGGTGTGGTGG-3'	Au NPs	DPV	100 fM - 2 mM	21 fM	[176]
Thrombin	GGGGTGACT-3'	Au NPs	DPV	0–1 ng mL ⁻¹	190 fg mL ⁻¹	[177]
Thrombin	5'-SH-(CH ₂) ₆ -GGTTGGTGTGGTGG-3'	Au NPs	DPV	0.1 pM - 10 nM	35 fM	[178]
Thrombin	Apt 1: 5'-SH-(CH ₂) ₆ -AGTCGGTGGTAGGGAGGTGGGGTGACT-3'	Hairbrush-like Au nanostructure	DPV	0.125–128 ng mL ⁻¹	50 pg mL ⁻¹	[179]
Prostate specific antigen (PSA)	Apt1: 5'-AAAAAAAAGGTGTGGTGGTGG-3'	Au NPs	DPV	0.1 pM - 10 nM	35 fM	[178]
Prostate specific antigen (PSA)	Apt2: 5'-AGTCGGTGGTAGGGAGGTGGGGTGACTGTGTAAGAAAGTGTG-3'	Hairbrush-like Au nanostructure	DPV	0.125–128 ng mL ⁻¹	50 pg mL ⁻¹	[179]
MCF-7 cells	5'-SH-(CH ₂) ₆ -GGTGGTGGTGGTGGTGGTGGTGG-3'	Au NPs/hydroxyapatite NR nanocomposite	DPV	10 - 10 ⁶ cells mL ⁻¹	8 cells mL ⁻¹	[27]
MCF-7 cells	5'-SH-CAGGCTACGGACAGTAGACATCACCATGATCCTG-3'	Au NPs	SWV	0.52–1.17 nM	0.52 nM	[29]
Mucin 1	5'-biotin- GGGAGACAAGATAACGGCTCAAGCAGTTGATCTTTGGATACCCCTGGT TCGACAGGAGGCTCACAACAGGC-3'	Au NPs/GO/PEDOT nanocomposite	DPV	3.13 aM - 31.25 nM	0.031 fM	[28]
human promyelocytic leukemia cells (HL- 60) cancer cells	5'-SH-(CH ₂) ₆ - ATCCAGATGACGAGCATGCCCTAGTACTACTACTCTTTTACGAAAGCCCTCG CTTTGGACACGGTGGCTTAGT-3'	Au/Ni/MnO ₂ /polyethylenimine (PEI) nanocomposite	EIS	2.5 × 10 ⁴ –5 × 10 ⁵ cells mL ⁻¹	250 cells mL ⁻¹	[180]
Tau381	5'-NH ₂ -GCGGAGCGTGGCAGG-3'	Carboxyl Graphene/Thionin/Au NPs nanocomposite	DPV	1.0–100 pM	0.70 pM	[167]
Immunoglobulin E	5'-SH-GGGGACAGTTTATCGTCCCTCTCTAGTGGGTGCCCC-3'	Macroporous Au nanostructure	DPV	5.52–10 pg mL ⁻¹	42 fg mL ⁻¹	[35]
TNF-α	5'-SH-(CH ₂) ₆ -TGGTGGATGGGAGTGGCGGACAA-3'	Au NPs	DPV	1–100 pg mL ⁻¹	0.52 pg mL ⁻¹	[160]
Dopamine	5'-SH-(CH ₂) ₆ -GGGAAUCCCGUGUGCCCGGGGAAAGAGGAAUUAUAGGCCAG CACAAUGUGAGGCCUCCUCC-3'	Spindle-shaped Au nanostructure	DPV	25 pg mL ⁻¹ - 3 ng mL ⁻¹	2 pg mL ⁻¹	[10]
Dopamine	5'-SH-(CH ₂) ₆ -GTCTCTGTGTGCGCCAGAGAACTGGGCGAGATATGGGCCAGCAC AGAAATGAGGCC-3'	rGO/nile blue/Au NPs nanocomposite	CV/DPV	10 nM - 0.2 mM	1 nM	[181]

led to a very high cost and also some health problems. DsrAB is a sulfite reductase related to SRB. So, determining the DsrAB genes can be used for the diagnosis of the corrosion induced by SRB. Here, a nanosheet containing 3-dimensional graphene (3D G) hierarchical structure functionalized with Au NPs was prepared and coated on the surface of a GCE to provide an enhanced surface area for immobilization of the biorecognition element. The capture probe (aptamer) was thiolated and could establish Au-S binding with the Au NPs. Then, the aptasensor was applied for a specified diagnosis of DsrAB DNA. In the presence of DsrAB DNA, aptamer was hybridized with it, and the peak current reduced gradually along with the concentration of the analyte. When the DsrAB DNA did not exist in the environment, the free, available, and active sites for redox reaction on the surface of the transducer were in a maximum status. However, in the presence of the analyte, due to the occurred hybridization between the aptamer and the analyte, the available sites for redox reaction were reduced along with increment the concentration of the analyte. The detection range for this aptasensor was 1.0×10^{-14} to 1.0×10^{-7} M, and the LOD was about 9.41×10^{-15} M. Tuberculous meningitis (TBM) is the primary form of tuberculosis that affects the central nervous system and is led to a high rate of death and disability. HspX antigen is related to *Mycobacterium tuberculosis* and considered as a reliable biomarker for the diagnosis of TBM [184]. In a research, an electrochemical aptasensor was designed for the diagnosis of HspX [185]. Here, a carbon screen-printed electrode was used as the transducer and modified with Au NPs. At the next step, a thiolated aptamer (3'-end-functionalized with thiol group) was immobilized on the surface of the modified electrode with Au NPs. The mentioned aptamer was also functionalized with MB as the redox marker from the 5'-end. In the absence of the analyte, the aptamer was free, and MB molecules created the maximum peak current, and electron transfer rate achieved from the surface of the transducer. While in the presence of HspX molecules, due to high affinity of aptamer against the target, the conformation of aptamer was changed and captured the HspX where this event was led to enhance the distance between the redox marker molecules and surface of transducer; this mechanism confirmed that the electrochemical current was decidedly weaker in the presence of HspX as the analyte. This signal-off aptasensor could determine the mentioned biomarker in a linear range from 0.01 to 500 ng mL⁻¹, and the LOD was about 10 pg mL⁻¹. Influenza is an acute respiratory infection that caused by influenza viruses. H1N1 is a virus associated to type A influenza virus. H1N1 is dangerous and can affect human health, especially children and the elderly. Rapid diagnosis of H1N1 can be beneficial in faster treatment as well as in preventing the spread of the disease. In a research, a new procedure was used to obtain aptamer sequences without polymerase chain reaction (PCR) amplification (Competitive non-SELEX) [186]. The authors of this research claimed that the obtained aptamers with this method could detect targets, among other existed similar structures. This advantage means that selectivity has increased dramatically. Then, the aptamer was applied as the biorecognition element in design an electrochemical aptasensor for the diagnosis of H1N1. This aptamer showed a high affinity against H1N1 ($K_D = 82$ pM). In this aptasensor, a disposable electrochemical printed (DEP) chip was applied as a three-electrode sensing system where the working electrode was carbon, and then a solution containing protein of H1N1 was dropped on it as the target. On the other hand, after the incubation process between the electrode and target molecules, the electrode was dried. Subsequently, a selected aptamer was conjugated with Au NPs and drooped on the surface of the chip. The electrochemical detection was based on the electrooxidation reaction of Au NPs; the DPV signal was increased when more Au NPs captured by the protein of H1N1 on the surface of the working electrode and the DPV was decreased when most of the protein of H1N1 were captured by aptamer strands in the solution (Fig. 7). This aptasensor could detect H1N1 in a dynamic range from 0.4 to 100 µg mL⁻¹, and the LOD was 0.51 µg mL⁻¹.

Tuberculosis is a common infectious disease, and deadly in many

cases. Different strains of *Mycobacteria* cause the disease, typically *Mycobacterium Tuberculosis* [187]. Tuberculosis typically attacks the lungs and can also affect other organs. Researchers believe one-third of the world's population is infected with *Mycobacterium Tuberculosis*. Therefore, rapid and accurate detection of this pathogen is essential. In a research, MPT64, as the antigen of *Mycobacterium Tuberculosis* was diagnosed by an electrochemical aptasensor equipped with Au@Prussian blue (PB) nanocomposite [38]. This nanocomposite was prepared using electrostatic adsorption between Au NPs and PB NPs. This adsorption was performed based on the stabilized surface charge provided by poly (diallyl dimethyl ammonium chloride) (PDDA). Afterward, Au@PB nanocomposite was conjugated with a thiolated aptamer (Apt2) and HRP, respectively. At this moment, the Au@PB-HRP-aptamer was achieved. At the next step, an Au electrode was applied as the working electrode, and another thiolated aptamer (Apt1) was immobilized on the surface of it. Then, the working electrode was filled in the presence of the analyte and captured it from one side; subsequently, Au@PB-HRP-aptamer was added and could capture the analyte from the other side. When the analyte existed, an enzymatic reaction catalyzed by HRP occurred where HQ oxidized to BQ, and in a mirror reaction H₂O₂ was reduced to H₂O. This enzymatic reaction was led to a change in output DPV signals along with the concentration of the analyte. This signal-on sandwich-like aptasensor was able to detect MPT64 in a range from 1 to 10,000 pg mL⁻¹ while the LOD was 21 fg mL⁻¹. Enterococci are important causes of nosocomial infections as well as common causes of urinary tract infections [188]. These bacteria are very diverse organisms and can survive in the environment or on the body of patients or others. *Enterococcus faecalis* is a type of bacteria that usually resists against many antibiotics [189]. In a research, an electrochemical aptasensor was designed based on an ice crystals-like Au nanostructure for the detection of *Enterococcus faecalis* gene sequence [190]. In the first step, in order to find an array of the Au nanostructure, a solution containing HAuCl₄, H₂SO₄, sorbitol, and deionized water was prepared; then, the synthesize solution was electrodeposited on the surface of an Au electrode via an amperometry procedure at 0 V for 5 min. Then, a thiolated aptamer (p-DNA, 35mer) was immobilized on the surface working electrode and a stable covalent Au-S bond established between ice crystals-like Au nanostructure and functionalized aptamer with thiol. Finally, the designed aptasensor was applied to determine the various concentrations of the analyte genome. Here, toluidine blue ($E^0 = -290$ mV) was applied as the redox marker. In the absence of analyte (c-DNA), a hydrophobic interaction occurred between the redox marker and aptamer and potential shifts to -278 mV; whereas, in the presence of c-DNA, due to high affinity of p-DNA, a hybridized double-strand structure of DNA was created that increased potential to -264 mV resulted from hydrophobic reactions of redox marker along with the concentrations of analyte. The results of this research confirmed that the redox marker was more strongly bound with the hybridized double-strand structure of DNA, and the reduction peak current was occurred along with increment the concentration of the analyte. This signal-off aptasensor could detect *Enterococcus faecalis* gene sequence in a linear range from 1×10^{-17} to 1×10^{-10} M, and the LOD was reported as 4.7×10^{-20} M. Table 4 shows the summary of recent researches based on Au nanostructure-based electrochemical aptasensors for the diagnosis of pathogens.

6. Analysis various type of electrochemical aptasensors based on the Au nanostructures

In this section, the essential features and components used in all the studied aptasensors were collected, ordered, and reviewed. Optimal diagnostic techniques are essential in the design of aptasensors. As shown in Fig. 8 (a), the DPV technique was used in most of the studied aptasensors (66%). One of the crucial advantages of this method is a high diagnostic sensitivity, applicability in inexpensive systems, short response times, and analytical investigation of redox processes

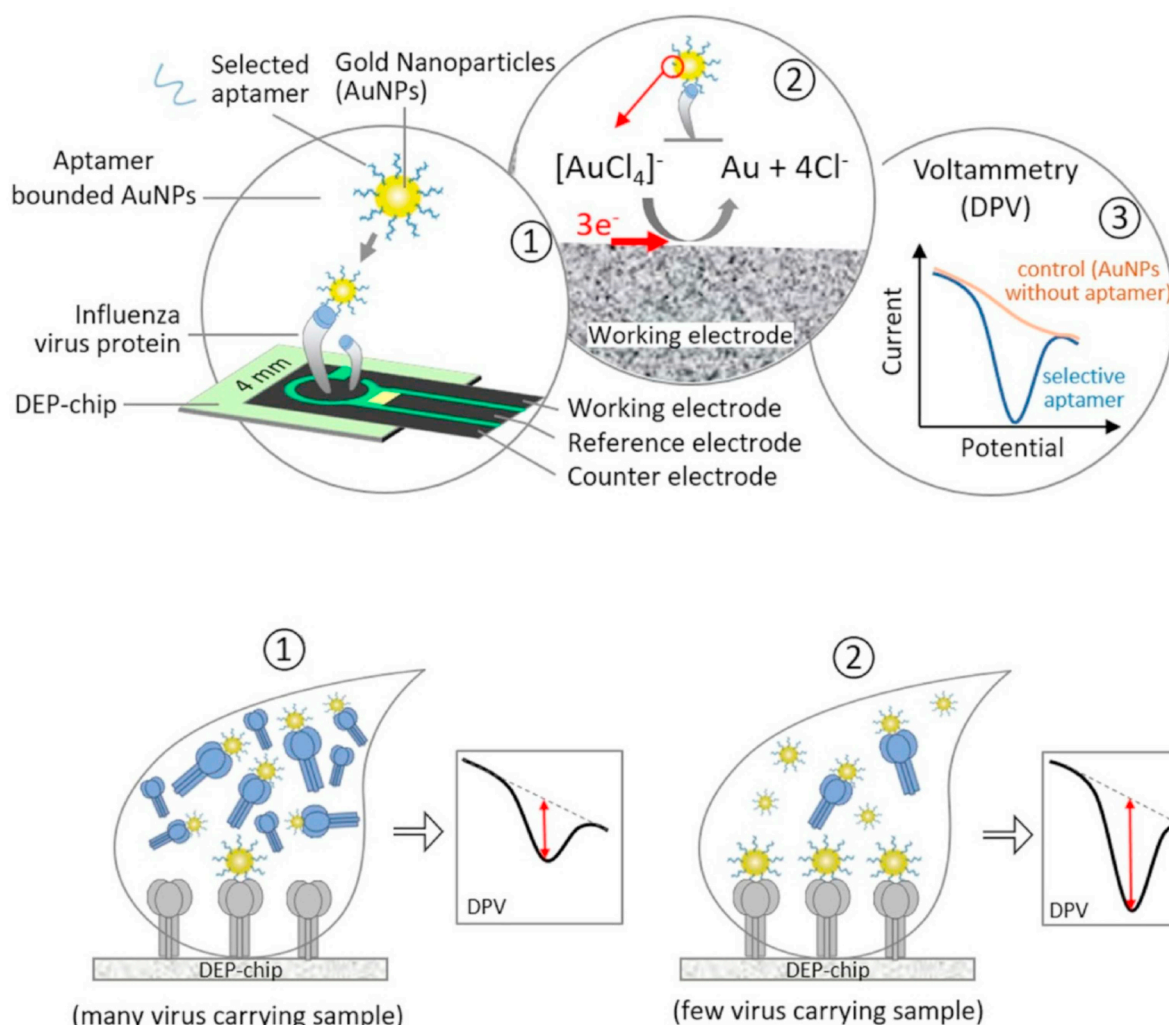


Fig. 7. Au NPs-based electrochemical aptasensor design steps to detect H1N1 virus; License Number: not applicable (open access).

occurring on the surface of the signal transducer. Besides, the EIS technique was used in 15% of the studied aptasensors. This technique has significant advantages such as acceptable sensitivity and providing characterizations and the capacity of electrochemical systems. Among the investigated aptasensors, the use of other diagnostic techniques was including of PEC, ECL, SWV, and CV. Functionalizing aptamers with different substances pursue different aims. These functionalizing agents are selected according to the surface in which the aptamer will be immobilized so that they can establish a stable and optimal attachment to the aptasensor components. Among the reviewed aptasensors, thiol was used in 74% of aptasensors and was able to create stable covalent bonding with Au molecules (Fig. 8 (b)). 20% of the aptamers studied were also functionalized with amines. It should be noted that biotin, disulfide, and carboxyl functional groups were also used to functionalize some aptamers used in aptasensors (Fig. 8 (b)). In all evaluated aptasensors in this review, after aptamer immobilization process, BSA, 1-Hexanthiol (1-HT), and MCH were used as the primary substances to block non-specific binding sites of aptamers. Choosing a signal transducer depends on many factors, such as the type of nanostructure to modify the surface, the type of functional group of biorecognition element, the kind of technique used in the assay, the stability and ease of use, and even the tact of the researcher. In this review, most of the studied aptasensors used the GCE electrode as the signal transducer (41%). About 35% of the studied aptasensors also used the Au electrode (GE: Au) as the signal transducer (Fig. 8 (c)). Other signal transducers

such as carbon electrode (CE), indium tin oxide electrode (ITO), fluorine tin oxide electrode (FTO), carbon paste electrode (CPE), titanium (Ti), pencil graphite electrode (PGE), and paper-based bipolar electrode (PBPE) were also applied in some aptasensors. All of the aptasensors studied in this review utilized Au nanostructures in their structure. One of the critical and applicable issues is the use of these Au nanostructures in two different locations. As shown in Fig. 8 (d), 77% of these Au nanostructures were used to modify the surface and increase the sensitivity of the signal transducer. These Au nanostructures on the surface of the signal transducer provided a suitable and stable space for interaction with the biorecognition element. In 23% of evaluated aptasensors, Au nanostructures were used in conjugation with other components of the biorecognition element. These nanostructures were commonly attached to aptamers and at a distance far from the surface of the signal transducer. In general, the use of Au nanostructures in the assembly of aptasensors has led to an increase in the active surfaces in diagnostic processes. Among the types of used Au nanostructures, Au nanocomposites were applied in 45% and pure Au NPs in 36%. In 19% of the cases, other arrays of Au nanostructures were used (Fig. 8, (e)). Overall, the use of Au nanostructures in different compounds and morphologies has been used to improve diagnostic sensitivity, increase the stability of aptasensor components, reduce costs, and speed up the detection time. In most evaluated aptasensors, the use of any nanostructure was significantly associated with the kind of signal transducer and functional group of aptamers.

Table 4
Au nanostructure-based electrochemical aptasensors for diagnosis of pathogens.

Type of pathogen	Aptamer sequence	Type of Au nanostructure	Detection technique	Detection range	LOD	Ref.
<i>Staphylococcus aureus</i>	5'-SH-TCCGACGTTCTCAGTAGCGCTCGCTGATCCACAGCTACGTC-3'	Au NPs/carbon nanoparticles (CNPs)/cellulose nanofibers nanocomposite	EIS	1.2×10^{11} - 1.2×10^8 CFU mL ⁻¹	1 CFU mL ⁻¹	[191]
<i>Shigella dysenteriae</i>	5'-ATAGAGCTACGACGACCGAACTAGCGTTTAAATGCCAGGACTGAAGTAGCGGAGTTAGTCAAGAGGTAGCGCACATA-3'	Au NPs	EIS	10^1 - 10^6 CFU mL ⁻¹	10^0 CFU mL ⁻¹	[192]
Salmonella Typhimurium	5'-SH-TATGGCGCGTCAACCGACGGGAGCTTGACATTAATGACA-G-3'	Nanoporous Au	EIS	6.5×10^2 - 6.5×10^8 CFU mL ⁻¹	1 CFU mL ⁻¹	[193]
Trichomonas vaginalis	5'-SH-(CH ₂) ₆ -TTTTTTTTTTCATGTGTCCTCCAAAGGCTAAGTACTGGGG-3'	Anisotropic-shaped Au NPs	DPV	1×10^{-19} - 1×10^{-12} M	3.1×10^{-20} M	[194]
dissimilatory sulfite reductase (DsrAB) gene of SRB	5'-SH-ACGTAGTTGTGTACGGGGCGGG-3'	Au NPs	DPV	1.0×10^{-14} - 1.0×10^{-7} M	9.41×10^{-15} M	[183]
<i>Salmonella typhimurium</i>	_____a	Au NPs	DPV	20 - 2×10^8 CFU mL ⁻¹	16 CFU mL ⁻¹	[195]
<i>Mycobacterium tuberculosis</i> antigen MPT64	Apt 1: 5'-SH-(CH ₂) ₆ -TGGGAGCTGATGTGCGATGGGTTTGTATCATCATGA-3'	Au NPs	DPV	0.02-1000 pg mL ⁻¹	10 fg mL ⁻¹	[38]
<i>Enterococcus faecalis</i>	Apt 2: 5'-SH-(CH ₂) ₆ -TTCCGGAAATGATTATCAAAATTTATGCCCTCTGAT-3'	Au NPs	DPV	1×10^{-17} - 1×10^{-10} M	4.7×10^{-20} M	[190]
<i>Escherichia coli</i> LPS	5'-SH-TTTTTTTTTTCAATTGGAAGAGGAGTGGCGGAGG-3'	Ice crystals-like Au nanostructure	DPV	0.1-0.9 pg mL ⁻¹	1 fg mL ⁻¹	[40]
	5'-NH ₂ C ₆ -CTTCTGCCGCGCTCTCTCTAGCCGATCGCGCTGGCCA GATGATA	rGO/Au NPs nanocomposite	DPV	1-10,000 pg mL ⁻¹	21 fg mL ⁻¹	[39]
<i>Mycobacterium tuberculosis</i> antigen MPT64	TAAAGGGTCAGCCCC CCAGGAGAGGAGATAGCGGACACT-3'	Au NPs	DPV	0.01-500 ng mL ⁻¹	10 pg mL ⁻¹	[185]
HspX Antigen	5'-SH-(CH ₂) ₆ -TGGGAGCTCATCTCGCATGGGTTTGTATCATCATGA-3'	Au NPs	DPV	0.4-100 µg mL ⁻¹	0.51 µg mL ⁻¹	[186]
	5'-MB-AGGGCTTTTTTTTTTTTAGTCTGTTTG-SH-(CH ₂) ₆ -3'					
	5'-TAGGTCGTACTCTGGCGGCGCTGTTTGGC-3'					

^a Sequence not reported.

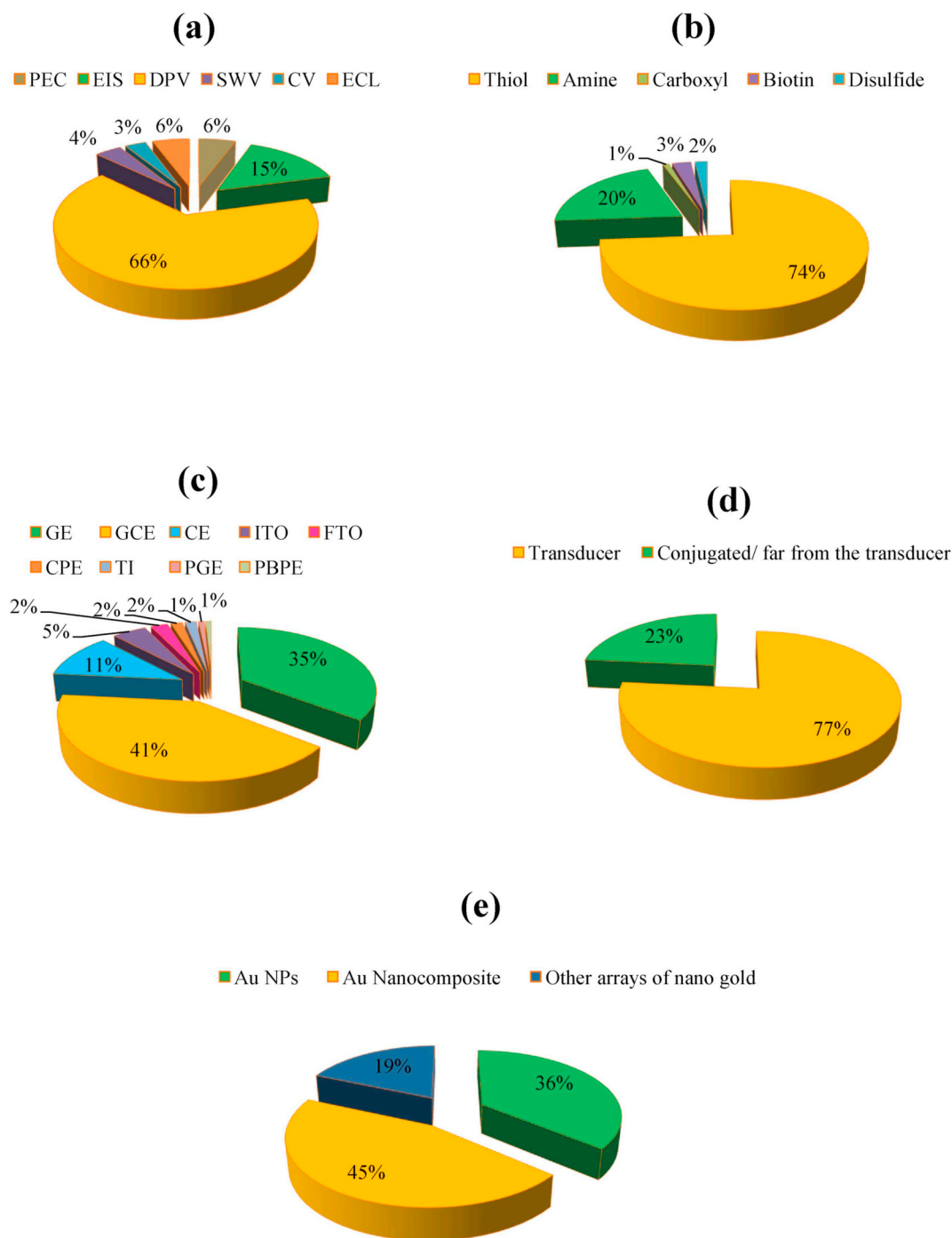


Fig. 8. Main features of evaluated electrochemical aptasensors: a) detection techniques; b) functional group of aptamers; c) type of transducers; d) location of Au nanostructures and e) type of applied Au nanostructures.

7. Conclusion

In the presented review, the various leading researches based on the electrochemical aptasensors have been investigated. The evaluated aptasensors used of GE, GCE, CE, ITO, FTO, CPE, TI, PGE and PBPE as the transducer. Specific aptamer strands were used as the biorecognition element and in order to reach the high affinity binding with the signal transducers or analytes, they were functionalized with thiol, amine, biotin, disulfide, and carboxyl functional groups. Au nanostructures with different sizes and morphologies were used in the presented aptasensors as the electron transfer facilitator and led to a

significant increment in the diagnostic sensitivity. It should be noted that Au nanostructures were used in pure or composite forms; the composite forms were in the presence of other types of nanostructures such as carbon or other nanomaterials. Diagnostic electrochemical techniques were different and, in most cases, were DPV and EIS. These aptasensors were able to detect analytes with higher specificity, higher stability, and lower LOD than other assay methods. Also, these aptasensors were able to show effective performance in detecting real samples. These aptasensors can be considered as an alternative and optimal method in the future of biomedical diagnostics.

8. Future perspectives

Au nanostructure-based electrochemical aptasensors can improve the accuracy, stability, and detection condition in biomedical diagnostics. Au nanostructures have significant advantages in the design of aptasensors, which has led to the development and optimization of these aptasensors. The use of aptamers as the biorecognition element in the structure of biosensors has led to specific detection of analytes. In future researches, aptamers may be designed and selected with high selectivity (~100%) against the analyte, and their stability (over current aptamers) may be increased. It is suggested that biosynthesis methods be used in the production of Au nanostructures in future researches, as well as the design of aptasensors to be followed in the presence of several nanostructures and the optimal combination be used for the synthesis of these nanostructures. Also, the nanostructures synthesis conditions should be optimized for each type of analyte. Simultaneous use of different signal transducers such as polycrystalline electrodes, screen-printed electrodes, etc. is suggested to find the most optimal signal transducer. The design of these aptasensors for the detection of critical analytes should not be confined to research laboratories and should provide an approach that can be rapidly utilized in combining electronic and computer sciences as optimum commercial aptasensors for the analyte detection. These efforts can make significant gains in promoting the survival rate and the quality of life.

Declaration of competing interest

The conflict of interest is not applicable when I am the sole author.

Acknowledgements

Foremost, I would like to express my sincere gratitude to Dr. H. Heli for the continuous support of my researches, for his patience, motivation, enthusiasm, and immense knowledge. His guidance helped me in all the time of study, research and writing (2015-2019). My sincere thanks also go to Dr. N. Sattarahmady, for offering me the many learning opportunities in her lab (Nanomedicine and Nanobiology Research Center, Shiraz University of Medical Sciences, Shiraz, Iran; 2015-2019).

References

- [1] A. Sadana, N. Sadana, *Handbook of Biosensors and Biosensor Kinetics*, Elsevier Science, 2010.
- [2] X. Zhang, H. Ju, J. Wang, *Electrochemical Sensors, Biosensors and Their Biomedical Applications*, Elsevier Science, 2011.
- [3] P. Yanez-Sedeno, J. Pingarron, Gold nanoparticle-based electrochemical biosensors, *Anal. Bioanal. Chem.* 382 (4) (2005) 884–886.
- [4] N.J. Ronkainen, H.B. Halsall, W.R. Heineman, *Electrochemical biosensors*, *Chem. Soc. Rev.* 39 (5) (2010) 1747–1763.
- [5] N. Wongkaew, M. Simsek, C. Griesche, A.J. Baeumner, Functional nanomaterials and nanostructures enhancing electrochemical biosensors and lab-on-a-chip performances: recent progress, applications, and future perspective, *Chem. Rev.* 119 (1) (2018) 120–194.
- [6] C.A. Borrebaeck, Antibodies in diagnostics—from immunoassays to protein chips, *Immunol. today* 21 (8) (2000) 379–382.
- [7] M. Negahdary, M. Behjati-Ardakani, N. Sattarahmady, H. Yadegari, H. Heli, Electrochemical aptasensing of human cardiac troponin I based on an array of gold nano dumb bells-Applied to early detection of myocardial infarction, *Sensor. Actuator. B Chem.* 252 (2017) 62–71.
- [8] M. Negahdary, H. Heli, An ultrasensitive electrochemical aptasensor for early diagnosis of Alzheimer's disease, using a fern leaves-like gold nanostructure, *Talanta* 198 (2019) 510–517.
- [9] M. Negahdary, M. Behjati-Ardakani, H. Heli, An electrochemical troponin T aptasensor based on the use of a macroporous gold nanostructure, *Microchimica Acta* 186 (6) (2019) 377.
- [10] R.A. Taheri, K. Eskandari, M. Negahdary, An electrochemical dopamine aptasensor using the modified Au electrode with spindle-shaped gold nanostructure, *Microchem. J.* 143 (2018) 243–251.
- [11] M. Negahdary, M. Behjati-Ardakani, N. Sattarahmady, H. Heli, An aptamer-based biosensor for troponin I detection in diagnosis of myocardial infarction, *J. Biomed. Phys. Eng.* 8 (2) (2018) 167.
- [12] M. Heiat, M. Negahdary, Sensitive diagnosis of alpha-fetoprotein by a label free nano apta sensor designed by modified Au electrode with spindle-shaped gold nanostructure, *Microchem. J.* 148 (2019) 456–466.
- [13] M. Negahdary, H. Heli, An electrochemical peptide-based biosensor for the Alzheimer biomarker amyloid- β (1–42) using a microporous gold nanostructure, *Microchimica Acta* 186 (12) (2019) 766.
- [14] M. Negahdary, H. Heli, An electrochemical troponin I peptisensor using a triangular icicle-like gold nanostructure, *Biochem. Eng. J.* 151 (2019) 107326.
- [15] Z. Yazdani, H. Yadegari, H. Heli, A molecularly imprinted electrochemical nanobiosensor for prostate specific antigen determination, *Anal. Biochem.* 566 (2019) 116–125.
- [16] A.A. Ensafi, *Electrochemical biosensors*, Elsevier, 2019.
- [17] N. Elgrishi, K.J. Rountree, B.D. McCarthy, E.S. Rountree, T.T. Eisenhart, J.L. Dempsey, A practical beginner's guide to cyclic voltammetry, *J. Chem. Educ.* 95 (2) (2018) 197–206.
- [18] F. Scholz, *Electroanalytical Methods: Guide to Experiments and Applications*, Springer Berlin Heidelberg, 2013.
- [19] F. Ciucci, Modeling electrochemical impedance spectroscopy, *Curr. Opin. Electrochem.* 13 (2018) 132–139.
- [20] V. Mirceski, D. Guziejewski, L. Stojanov, R. Gulaboski, Differential square-wave voltammetry, *Anal. Chem.* 91 (23) (2019) 14904–14910.
- [21] X. Liu, P. Liu, Y. Tang, L. Yang, L. Li, Z. Qi, D. Li, D.K.Y. Wong, A photoelectrochemical aptasensor based on a 3D flower-like TiO₂-MoS₂-gold nanoparticle heterostructure for detection of kanamycin, *Biosens. Bioelectron.* 112 (2018) 193–201.
- [22] W.-J. Zeng, N. Liao, Y.-M. Lei, J. Zhao, Y.-Q. Chai, R. Yuan, Y. Zhuo, Hemin as electrochemically regenerable co-reaction accelerator for construction of an ultrasensitive PTCA-based electrochemiluminescent aptasensor, *Biosens. Bioelectron.* 100 (2018) 490–496.
- [23] M. Adeel, M.M. Rahman, J.-J. Lee, Label-free aptasensor for the detection of cardiac biomarker myoglobin based on gold nanoparticles decorated boron nitride nanosheets, *Biosens. Bioelectron.* 126 (2019) 143–150.
- [24] X. Cao, J. Xu, J. Xia, F. Zhang, Z. Wang, An electrochemical aptasensor based on the conversion of liquid-phase colorimetric assay into electrochemical analysis for sensitive detection of lysozyme, *Sensor. Actuator. B Chem.* 255 (2018) 2136–2142.
- [25] Z. Cao, F. Duan, X. Huang, Y. Liu, N. Zhou, L. Xia, Z. Zhang, M. Du, A multiple aptasensor for ultrasensitive detection of miRNAs by using covalent-organic framework nanowire as platform and shell-encoded gold nanoparticles as signal labels, *Anal. Chim. Acta* 1082 (2019) 176–185.
- [26] J. Chen, W. Hu, J. Wei, F. Yu, L. Wu, C. Wang, W. Wang, S. Zuo, B. Shang, Q. Chen, An electrochemical aptasensing platform for carbohydrate antigen 125 based on the use of flower-like gold nanostructures and target-triggered strand displacement amplification, *Microchimica Acta* 186 (6) (2019) 388.
- [27] L. Farzin, M. Shamsipur, L. Samandari, S. Sheibani, Signalling probe displacement electrochemical aptasensor for malignant cell surface nucleolin as a breast cancer biomarker based on gold nanoparticle decorated hydroxyapatite nanorods and silver nanoparticle labels, *Microchimica Acta* 185 (2) (2018) 154.
- [28] P. Gupta, A. Bharti, N. Kaur, S. Singh, N. Prabhakar, An electrochemical aptasensor based on gold nanoparticles and graphene oxide doped poly(3,4-ethylenedioxythiophene) nanocomposite for detection of MUC1, *J. Electroanal. Chem.* 813 (2018) 102–108.
- [29] M. Hasanazadeh, N. Razmi, A. Mokhtarzadeh, N. Shadjou, S. Mahboob, Aptamer based assay of plated-derived growth factor in unprocessed human plasma sample and MCF-7 breast cancer cell lysates using gold nanoparticle supported α -cyclodextrin, *Int. J. Biol. Macromol.* 108 (2018) 69–80.
- [30] C. Ibañ, M.K. Md Arshad, S.C.B. Gopinath, M. Nuzaihan, M.N. M.F.M. Fathil, P. Estrela, Gold interdigitated triple-microelectrodes for label-free prognostic aptasensing of prostate cancer biomarker in serum, *Biosens. Bioelectron.* 136 (2019) 118–127.
- [31] Z. Li, J. Yin, C. Gao, G. Qiu, A. Meng, Q. Li, The construction of electrochemical aptasensor based on coral-like poly-aniline and Au nano-particles for the sensitive detection of prostate specific antigen, *Sensor. Actuator. B Chem.* 295 (2019) 93–100.
- [32] P.F. Rostamabadi, E. Heydari-Bafrooei, Impedimetric aptasensing of the breast cancer biomarker HER2 using a glassy carbon electrode modified with gold nanoparticles in a composite consisting of electrochemically reduced graphene oxide and single-walled carbon nanotubes, *Microchimica Acta* 186 (8) (2019) 495.
- [33] M. Saremi, A. Amini, H. Heydari, An aptasensor for troponin I based on the aggregation-induced electrochemiluminescence of nanoparticles prepared from a cyclometallated iridium(III) complex and poly(4-vinylpyridine-co-styrene) deposited on nitrogen-doped graphene, *Microchimica Acta* 186 (4) (2019) 254.
- [34] F. Shahdost-fard, M. Roushani, Designing of an Ultrasensitive BCM-7 Aptasensor Based on an SPCE Modified with AuNR for Promising Distinguishing of Autism Disorder, *Talanta*, 2019, p. 120506.
- [35] Y. Wang, M. Cui, M. Jiao, X. Luo, Antifouling and ultrasensitive biosensing interface based on self-assembled peptide and aptamer on macroporous gold for electrochemical detection of immunoglobulin E in serum, *Anal. Bioanal. Chem.* 410 (23) (2018) 5871–5878.
- [36] Y. Wang, J. Luo, J. Liu, S. Sun, Y. Xiong, Y. Ma, S. Yan, Y. Yang, H. Yin, X. Cai, Label-free microfluidic paper-based electrochemical aptasensor for ultrasensitive and simultaneous multiplexed detection of cancer biomarkers, *Biosens. Bioelectron.* 136 (2019) 84–90.
- [37] S. Yang, M. You, F. Zhang, Q. Wang, P. He, A sensitive electrochemical aptasensing platform based on exonuclease recycling amplification and host-guest recognition for detection of breast cancer biomarker HER2, *Sensor. Actuator. B Chem.* 258 (2018) 796–802.

- [38] N. Li, X. Huang, D. Sun, W. Yu, W. Tan, Z. Luo, Z. Chen, Dual-aptamer-based voltammetric biosensor for the Mycobacterium tuberculosis antigen MPT64 by using a gold electrode modified with a peroxidase loaded composite consisting of gold nanoparticles and a Zr(IV)/terephthalate metal-organic framework, *Microchimica Acta* 185 (12) (2018) 543.
- [39] N. Li, X. Huang, D. Sun, Y. Zhong, Z. Chen, A sensitive and rapid electrochemical aptasensor based on Au@ PB for selective detection of Mycobacterium tuberculosis antigen MPT64, *J. Electrochem. Soc.* 166 (8) (2019) B604–B609.
- [40] M. Pourmadadi, J.S. Shayeh, M. Omid, F. Yazdian, M. Alebouyeh, L. Tayebi, A glassy carbon electrode modified with reduced graphene oxide and gold nanoparticles for electrochemical aptasensing of lipopolysaccharides from *Escherichia coli* bacteria, *Microchimica Acta* 186 (12) (2019) 787.
- [41] M. Sypabekova, P. Jolly, P. Estrela, D. Kanayeva, Electrochemical aptasensor using optimized surface chemistry for the detection of Mycobacterium tuberculosis secreted protein MPT64 in human serum, *Biosens. Bioelectron.* 123 (2019) 141–151.
- [42] W. Chen, C. Yan, L. Cheng, L. Yao, F. Xue, J. Xu, An ultrasensitive signal-on electrochemical aptasensor for ochratoxin A determination based on DNA controlled layer-by-layer assembly of dual gold nanoparticle conjugates, *Biosens. Bioelectron.* 117 (2018) 845–851.
- [43] S.H. Jalalian, M. Ramezani, N.M. Danesh, M. Alibolandi, K. Abnous, S.M. Taghdisi, A novel electrochemical aptasensor for detection of aflatoxin M1 based on target-induced immobilization of gold nanoparticles on the surface of electrode, *Biosens. Bioelectron.* 117 (2018) 487–492.
- [44] S. Mousavi Nodoushan, N. Nasirizadeh, J. Amani, R. Halabian, A.A. Imani Fooladi, An electrochemical aptasensor for staphylococcal enterotoxin B detection based on reduced graphene oxide and gold nano-urchins, *Biosens. Bioelectron.* 127 (2019) 221–228.
- [45] S. Mousavi Nodoushan, N. Nasirizadeh, R. Kachuei, A.A. Imani Fooladi, Electrochemical Detection of Aflatoxin B1; an Aptasensor prepared using graphene oxide and gold nanowires, *Anal. Method.* 11 (47) (2019) 6033–6042.
- [46] G. Peng, X. Li, F. Cui, Q. Qiu, X. Chen, H. Huang, Aflatoxin B1 electrochemical aptasensor based on tetrahedral DNA nanostructures functionalized three dimensionally ordered macroporous MoS₂-AuNPs film, *ACS Appl. Mater. Interfaces* 10 (21) (2018) 17551–17559.
- [47] Y. Tang, X. Liu, H. Zheng, L. Yang, L. Li, S. Zhang, Y. Zhou, S. Alwarappan, A photoelectrochemical aptasensor for aflatoxin B1 detection based on an energy transfer strategy between Ce-TiO₂@MoSe₂ and Au nanoparticles, *Nanoscale* 11 (18) (2019) 9115–9124.
- [48] C. Wang, H. Zhang, X. Jiang, B. Zhou, Electrochemical determination of aflatoxin B1 (AFB1) using a copper-based metal-organic framework (Cu-MOF) and gold nanoparticles (AuNPs) with exonuclease III (exo III) assisted recycling by differential pulse voltammetry (DPV), *Anal. Lett.* 52 (16) (2019) 2439–2453.
- [49] F. Wang, Y. Han, S. Wang, Z. Ye, L. Wei, L. Xiao, Single-particle LRET aptasensor for the sensitive detection of aflatoxin B1 with upconversion nanoparticles, *Anal. Chem.* 91 (18) (2019) 11856–11863.
- [50] P. Wang, L. Wang, M. Ding, M. Pei, W. Guo, Ultrasensitive electrochemical detection of ochratoxin A based on signal amplification by one-pot synthesized flower-like PEDOT-AuNFs supported on a graphene oxide sponge, *Analyst* 144 (19) (2019) 5866–5874.
- [51] S.S. Wu, M. Wei, W. Wei, Y. Liu, S. Liu, Electrochemical aptasensor for aflatoxin B1 based on smart host-guest recognition of β -cyclodextrin polymer, *Biosens. Bioelectron.* 129 (2019) 58–63.
- [52] A. Yagati, S. Chavan, C. Baek, M.-H. Lee, J. Min, Label-free impedance sensing of aflatoxin B1 with polyaniline nanofibers/Au nanoparticle electrode array, *Sensors* 18 (5) (2018) 1320.
- [53] X. Yang, D. Shi, S. Zhu, B. Wang, X. Zhang, G. Wang, Portable Aptasensor of aflatoxin B1 in bread based on a personal glucose meter and DNA walking machine, *ACS Sens.* 3 (7) (2018) 1368–1375.
- [54] H. Zejli, K.Y. Goud, J.L. Marty, Label free aptasensor for ochratoxin A detection using polythiophene-3-carboxylic acid, *Talanta* 185 (2018) 513–519.
- [55] J. Ding, D. Zhang, Y. Liu, M. Yu, X. Zhan, D. Zhang, P. Zhou, An electrochemical aptasensor for detection of lead ions using a screen-printed carbon electrode modified with Au/polypyrrole composites and toluidine blue, *Anal. Method.* 11 (33) (2019) 4274–4279.
- [56] Z. Chen, G. Lai, S. Liu, A. Yu, Ultrasensitive electrochemical aptasensing of kanamycin antibiotic by enzymatic signal amplification with a horseradish peroxidase-functionalized gold nanoprobe, *Sensor. Actuator. B Chem.* 273 (2018) 1762–1767.
- [57] S. Huang, N. Gan, T. Li, Y. Zhou, Y. Cao, Y. Dong, Electrochemical aptasensor for multi-antibiotics detection based on endonuclease and exonuclease assisted dual recycling amplification strategy, *Talanta* 179 (2018) 28–36.
- [58] S. Jafari, M. Dehghani, N. Nasirizadeh, M. Azimzadeh, An azithromycin electrochemical sensor based on an aniline MIP film electropolymerized on a gold nano urchins/graphene oxide modified glassy carbon electrode, *J. Electroanal. Chem.* 829 (2018) 27–34.
- [59] F. Li, X. Wang, X. Sun, Y. Guo, Multiplex electrochemical aptasensor for detecting multiple antibiotics residues based on carbon fiber and mesoporous carbon-gold nanoparticles, *Sensor. Actuator. B Chem.* 265 (2018) 217–226.
- [60] F. Li, X. Wang, X. Sun, Y. Guo, W. Zhao, A dual-signal amplification strategy for kanamycin based on ordered mesoporous carbon-chitosan/gold nanoparticles-streptavidin and ferrocene labelled DNA, *Anal. Chim. Acta* 1033 (2018) 185–192.
- [61] A. Mohammad-Razdari, M. Ghasemi-Varnamkhasti, Z. Izadi, A.A. Ensafi, S. Rostami, M. Siadat, An impedimetric aptasensor for ultrasensitive detection of Penicillin G based on the use of reduced graphene oxide and gold nanoparticles, *Microchimica Acta* 186 (6) (2019) 372.
- [62] Y. Sun, X. Jiang, H. Jin, R. Gui, Ketjen black/ferrocene dual-doped MOFs and aptamer-coupling gold nanoparticles used as a novel ratiometric electrochemical aptasensor for vanillin detection, *Anal. Chim. Acta* 1083 (2019) 101–109.
- [63] A. Sassolas, L.J. Blum, B.D. Leca-Bouvier, Electrochemical aptasensors, electroanalysis, *An Int. J. Devote. Fundam. Prac. Aspect. Electroanal.* 21 (11) (2009) 1237–1250.
- [64] M. Mascini, Aptamers in Bioanalysis, Wiley, 2009.
- [65] M. Negahdary, Aptamers in nanostructure-based electrochemical biosensors for cardiac biomarkers and cancer biomarkers: a review, *Biosens. Bioelectron.* 152 (2020) 112018.
- [66] G. Zon, Aptamers and clinical applications, *Adv. Nucleic Acid Therapeut.* 68 (2019) 367.
- [67] H. Kaur, J.G. Bruno, A. Kumar, T.K. Sharma, Aptamers in the therapeutics and diagnostics pipelines, *Theranostics* 8 (15) (2018) 4016.
- [68] S. Song, L. Wang, J. Li, C. Fan, J. Zhao, Aptamer-based biosensors, *Trac. Trends Anal. Chem.* 27 (2) (2008) 108–117.
- [69] J.-O. Lee, H.-M. So, E.-K. Jeon, H. Chang, K. Won, Y.H. Kim, Aptamers as molecular recognition elements for electrical nanobiosensors, *Anal. Bioanal. Chem.* 390 (4) (2008) 1023–1032.
- [70] S. Tombelli, M. Minunni, M. Mascini, Analytical applications of aptamers, *Biosens. Bioelectron.* 20 (12) (2005) 2424–2434.
- [71] W. Tan, H. Wang, Y. Chen, X. Zhang, H. Zhu, C. Yang, R. Yang, C. Liu, Molecular aptamers for drug delivery, *Trends Biotechnol.* 29 (12) (2011) 634–640.
- [72] K.-M. Song, S. Lee, C. Ban, Aptamers and their biological applications, *Sensors* 12 (1) (2012) 612–631.
- [73] Y. Dong, Aptamers for Analytical Applications: Affinity Acquisition and Method Design, Wiley 2019.
- [74] T.A. Rangrez, M.I. Ahamed, A.M. Asiri, Biosensors - Materials and Applications, Materials Research Forum LLC, 2019.
- [75] F. Du, L. Guo, Q. Qin, X. Zheng, G. Ruan, J. Li, G. Li, Recent advances in aptamer-functionalized materials in sample preparation, *Trac. Trends Anal. Chem.* 67 (2015) 134–146.
- [76] N.L. Rosi, C.A. Mirkin, Nanostructures in biodiagnostics, *Chem. Rev.* 105 (4) (2005) 1547–1562.
- [77] C.J. Delerue, M. Lannoo, Nanostructures: Theory and Modeling, Springer Science & Business Media, 2013.
- [78] G. Cao, Y. Wang, Nanostructures and Nanomaterials: Synthesis, Properties, and Applications, second ed., World Scientific Publishing Company, 2011.
- [79] O. de Oliveira, M. Ferreira, A.L. Da Róz, F. de Lima Leite, Nanostructures, Elsevier Science, 2016.
- [80] M. Hu, J. Chen, Z.-Y. Li, L. Au, G.V. Hartland, X. Li, M. Marquez, Y. Xia, Gold nanostructures: engineering their plasmonic properties for biomedical applications, *Chem. Soc. Rev.* 35 (11) (2006) 1084–1094.
- [81] C.M. Cobley, J. Chen, E.C. Cho, L.V. Wang, Y. Xia, Gold nanostructures: a class of multifunctional materials for biomedical applications, *Chem. Soc. Rev.* 40 (1) (2011) 44–56.
- [82] Y. Zhang, W. Chu, A.D. Foroushani, H. Wang, D. Li, J. Liu, C.J. Barrow, X. Wang, W. Yang, New gold nanostructures for sensor applications: a review, *Materials* 7 (7) (2014) 5169–5201.
- [83] Y. Zhang, G. Wang, L. Yang, F. Wang, A. Liu, Recent advances in gold nanostructures based biosensing and bioimaging, *Coord. Chem. Rev.* 370 (2018) 1–21.
- [84] S. Ebrahimi, R.E. Nahli, Nano-biosensors and Nano-Aptasensors for Stimulant Detection, *Environmental Nanotechnology*, Springer, 2019, pp. 169–193.
- [85] J.M. Blair, M.A. Webber, A.J. Baylay, D.O. Ogbolu, L.J. Piddock, Molecular mechanisms of antibiotic resistance, *Nat. Rev. Microbiol.* 13 (1) (2015) 42–51.
- [86] G. Lancini, F. Parenti, Antibiotics: an Integrated View, Springer Science & Business Media 2013.
- [87] B. He, L. Wang, X. Dong, X. Yan, M. Li, S. Yan, D. Yan, Aptamer-based thin film gold electrode modified with gold nanoparticles and carboxylated multi-walled carbon nanotubes for detecting oxytetracycline in chicken samples, *Food Chem.* 300 (2019) 125179.
- [88] X. Wang, D. Ryu, R.H. Houtkooper, J. Auwerx, Antibiotic use and abuse: a threat to mitochondria and chloroplasts with impact on research, health, and environment, *Bioessays* 37 (10) (2015) 1045–1053.
- [89] K.D. Rainsford, Ibuprofen: Discovery, Development and Therapeutics, 2015 Wiley.
- [90] M. Roushani, F. Shahdost-fard, Applicability of AuNPs@N-GQDs nanocomposite in the modeling of the amplified electrochemical Ibuprofen aptasensing assay by monitoring of riboflavin, *Bioelectrochemistry* 126 (2019) 38–47.
- [91] R.A. Goldstein, C. DesLauriers, A. Burda, K. Johnson-Arbor, Cocaine: history, social implications, and toxicity: a review, *Seminars in Diagnostic Pathology*, Elsevier, 2009, pp. 10–17.
- [92] N. Tavakkoli, N. Soltani, F. Mohammadi, A nanoporous gold-based electrochemical aptasensor for sensitive detection of cocaine, *RSC Adv.* 9 (25) (2019) 14296–14301.
- [93] N.J. Walton, M.J. Mayer, A. Narbad, Vanillin, *Phytochemistry* 63 (5) (2003) 505–515.
- [94] D. Norbäck, G. Wieslander, Biomarkers and chemosensory irritations, *Int. Arch. Occup. Environ. Health* 75 (5) (2002) 298–304.
- [95] E. Osserman, Lysozyme, Elsevier, 2012.
- [96] Z. Chen, Q. Xu, G. Tang, S. Liu, S. Xu, X. Zhang, A facile electrochemical aptasensor for lysozyme detection based on target-induced turn-off of photo-sensitization, *Biosens. Bioelectron.* 126 (2019) 412–417.
- [97] T.L. Rižner, W. Jäger, C. Özvey-Laczka, Relevance of Steroid Biosynthesis, Metabolism and Transport in Pathophysiology and Drug Discovery, *Frontiers Media SA*, 2019.
- [98] X. Liu, K. Deng, H. Wang, C. Li, S. Zhang, H. Huang, Aptamer based ratiometric electrochemical sensing of 17 β -estradiol using an electrode modified with gold

- nanoparticles, thionine, and multiwalled carbon nanotubes, *Microchimica Acta* 186 (6) (2019) 347.
- [99] A.R. Saltiel, J.E. Pessin, *Mechanisms of Insulin Action*, Springer New York, 2007.
- [100] Y. Zhao, Y. Xu, M. Zhang, J. Xiang, C. Deng, H. Wu, An electrochemical dual-signaling aptasensor for the ultrasensitive detection of insulin, *Anal. Biochem.* 573 (2019) 30–36.
- [101] A. Azadbakht, A.R. Abbasi, Impedimetric aptasensor for kanamycin by using carbon nanotubes modified with MoSe₂ nanoflowers and gold nanoparticles as signal amplifiers, *Microchimica Acta* 186 (1) (2018) 23.
- [102] B. He, S. Yan, Voltammetric kanamycin aptasensor based on the use of thionine incorporated into Au@Pt core-shell nanoparticles, *Microchimica Acta* 186 (2) (2019) 77.
- [103] J. Wang, K. Ma, H. Yin, Y. Zhou, S. Ai, Aptamer based voltammetric determination of ampicillin using a single-stranded DNA binding protein and DNA functionalized gold nanoparticles, *Microchimica Acta* 185 (1) (2017) 68.
- [104] Z. Liu, Q. Xu, J. Fu, Z. Shi, Q. Yang, Y. Guo, Y. Zhang, X. Sun, Z. Wang, Dual-signal amplification strategy aptasensor based on exonuclease III and ordered mesoporous carbon-gold nanocomposites for tetracycline detection in milk, *INT. J. ELECTROCHEM. SCI.* 13 (8) (2018) 8260–8274.
- [105] M. Roushani, K. Ghanbari, A novel aptasensor based on gold nanorods/ZnS QDs-modified electrode for evaluation of streptomycin antibiotic, *Anal. Method.* 10 (43) (2018) 5197–5204.
- [106] B. He, M. Li, A novel electrochemical aptasensor based on gold electrode decorated Ag@Au core-shell nanoparticles for sulfamethazine determination, *Anal. Bioanal. Chem.* 410 (29) (2018) 7671–7678.
- [107] B. He, G. Du, Novel electrochemical aptasensor for ultrasensitive detection of sulfadiazine based on covalently linked multi-walled carbon nanotubes and in situ synthesized gold nanoparticle composites, *Anal. Bioanal. Chem.* 410 (12) (2018) 2901–2910.
- [108] O.K. Okoth, K. Yan, J. Feng, J. Zhang, Label-free photoelectrochemical aptasensing of diclofenac based on gold nanoparticles and graphene-doped CdS, *Sensor. Actuator. B Chem.* 256 (2018) 334–341.
- [109] H.A. Samie, M. Arvand, Label-free electrochemical aptasensor for progesterone detection in biological fluids, *Bioelectrochemistry* 133 (2020) 107489.
- [110] X. Chen, Z. Guo, Y. Tang, Y. Shen, P. Miao, A highly sensitive gold nanoparticle-based electrochemical aptasensor for theophylline detection, *Anal. Chim. Acta* 999 (2018) 54–59.
- [111] M. Hosseini Ghalehno, M. Mirzaei, M. Torkzadeh-Mahani, Electrochemical aptasensor for activated protein C using a gold nanoparticle – chitosan/graphene paste modified carbon paste electrode, *Bioelectrochemistry* 130 (2019) 107322.
- [112] N. Wang, H. Dai, L. Sai, H. Ma, M. Lin, Copper ion-assisted gold nanoparticle aggregates for electrochemical signal amplification of lipopolysaccharide sensing, *Biosens. Bioelectron.* 126 (2019) 529–534.
- [113] A. Farzadfar, J.S. Shayeh, M. Habibi-Rezaei, M. Omid, Modification of reduced graphene/Au-aptamer to develop an electrochemical based aptasensor for measurement of glycated albumin, *Talanta* 211 (2020) 120722.
- [114] H. Beitollahi, R. Zaimbashi, M.T. Mahani, S. Tajik, A label-free aptasensor for highly sensitive detection of homocysteine based on gold nanoparticles, *Bioelectrochemistry* 134 (2020) 107497.
- [115] Y. Lv, Y. Zhou, H. Dong, L. Liu, G. Mao, Y. Zhang, M. Xu, Amplified electrochemical aptasensor for sialic acid based on carbon-cloth-supported gold nanodendrites and functionalized gold nanoparticles, *ChemElectroChem* 7 (4) (2020) 922–927.
- [116] L. Goldblatt, *Aflatoxin: Scientific Background, Control, and Implications*, Elsevier 2012.
- [117] M. Negahdary, H. Heli, Applications of nanoflowers in biomedicine, *Recent Patents on Nanotechnol.* 12(1) (2018) 22–33.t.
- [118] Z. Han, Z. Tang, K. Jiang, Q. Huang, J. Meng, D. Nie, Z. Zhao, Dual-target electrochemical aptasensor based on co-reduced molybdenum disulfide and Au NPs (rMoS₂-Au) for multiplex detection of mycotoxins, *Biosens. Bioelectron.* 150 (2020) 111894.
- [119] E.P. Preece, F.J. Hardy, B.C. Moore, M. Bryan, A review of microcystin detections in Estuarine and Marine waters: environmental implications and human health risk, *Harmful Algae* 61 (2017) 31–45.
- [120] X. Liu, Y. Tang, P. Liu, L. Yang, L. Li, Q. Zhang, Y. Zhou, M.Z.H. Khan, A highly sensitive electrochemical aptasensor for detection of microcystin-LR based on a dual signal amplification strategy, *Analyst* 144 (5) (2019) 1671–1678.
- [121] S. Kempahanumakkagari, A. Deep, K.-H. Kim, S.K. Kailasa, H.-O. Yoon, Nanomaterial-based electrochemical sensors for arsenic-A review, *Biosens. Bioelectron.* 95 (2017) 106–116.
- [122] A.A. Ensafi, F. Akbarian, E. Heydari-Soureshjani, B. Rezaei, A novel aptasensor based on 3D-reduced graphene oxide modified gold nanoparticles for determination of arsenite, *Biosens. Bioelectron.* 122 (2018) 25–31.
- [123] J.R. Rochester, Bisphenol A and human health: a review of the literature, *Reprod. Toxicol.* 42 (2013) 132–155.
- [124] I. Razavipannah, G.H. Rounaghi, B. Deiminat, S. Damirchi, K. Abnous, M. Izadyar, M. Khavani, A new electrochemical aptasensor based on MWCNT-SiO₂@Au core-shell nanocomposite for ultrasensitive detection of bisphenol A, *Microchem. J.* 146 (2019) 1054–1063.
- [125] P. Mitra, S. Sharma, P. Purohit, P. Sharma, Clinical and molecular aspects of lead toxicity: an update, *Crit. Rev. Clin. Lab Sci.* 54 (7–8) (2017) 506–528.
- [126] Y. Wang, G. Zhao, Q. Zhang, H. Wang, Y. Zhang, W. Cao, N. Zhang, B. Du, Q. Wei, Electrochemical aptasensor based on gold modified graphene nanocomposite with different morphologies for ultrasensitive detection of Pb²⁺, *Sensor. Actuator. B Chem.* 288 (2019) 325–331.
- [127] R.A. Bernhoft, Mercury toxicity and treatment: a review of the literature, *J. Environ. Pub. Health* (2012) 2012.
- [128] L. Zhao, Y. Wang, G. Zhao, N. Zhang, Y. Zhang, X. Luo, B. Du, Q. Wei, Electrochemical aptasensor based on Au@HS-rGO and thymine-Hg²⁺ + thymine structure for sensitive detection of mercury ion, *J. Electroanal. Chem.* 848 (2019) 113308.
- [129] M. Roushani, B. Zare Dizajdizi, Z. Rahmati, A. Azadbakht, Development of electrochemical aptasensor based on gold nanorod and its application for detection of aflatoxin B1 in rice and blood serum sample, *Nanochem. Res.* 4 (1) (2019) 35–42.
- [130] C. Gu, L. Yang, M. Wang, N. Zhou, L. He, Z. Zhang, M. Du, A bimetallic (Cu-Co) Prussian Blue analogue loaded with gold nanoparticles for impedimetric aptasensing of ochratoxin a, *Microchimica Acta* 186 (6) (2019) 343.
- [131] J. Xu, X. Qiao, Y. Wang, Q. Sheng, T. Yue, J. Zheng, M. Zhou, Electrostatic assembly of gold nanoparticles on black phosphorus nanosheets for electrochemical aptasensing of patulin, *Microchimica Acta* 186 (4) (2019) 238.
- [132] G. Xu, J. Hou, Y. Zhao, J. Bao, M. Yang, H. Fa, Y. Yang, L. Li, D. Huo, C. Hou, Dual-signal aptamer sensor based on polydopamine-gold nanoparticles and exonuclease I for ultrasensitive malathion detection, *Sensor. Actuator. B Chem.* 287 (2019) 428–436.
- [133] C. Zhu, D. Liu, Z. Chen, L. Li, T. You, An ultra-sensitive aptasensor based on carbon nanohorns/gold nanoparticles composites for impedimetric detection of carbendazim at picogram levels, *J. Colloid Interface Sci.* 546 (2019) 92–100.
- [134] A.A. Ensafi, M. Amini, B. Rezaei, Molecularly imprinted electrochemical aptasensor for the attomolar detection of bisphenol A, *Microchimica Acta* 185 (5) (2018) 265.
- [135] J. Yao, C. Liu, M. Yang, An ultrasensitive and highly selective electrochemical aptasensor for environmental endocrine disrupter bisphenol A determination using gold nanoparticles/nitrogen, sulfur, and phosphorus Co-doped carbon dots as signal enhancer and its electrochemical kinetic research, *J. Electrochem. Soc.* 166 (13) (2019) B1161–B1170.
- [136] M. Baghayeri, R. Ansari, M. Nodehi, I. Razavipannah, H. Veisi, Voltammetric aptasensor for bisphenol A based on the use of a MWCNT/Fe₃O₄@gold nanocomposite, *Microchimica Acta* 185 (7) (2018) 320.
- [137] M. Baghayeri, R. Ansari, M. Nodehi, I. Razavipannah, H. Veisi, Label-free electrochemical bisphenol A aptasensor based on designing and fabrication of a magnetic gold nanocomposite, *Electroanalysis* 30 (9) (2018) 2160–2166.
- [138] C. Hongxia, H. Ji, L. Zaijun, L. Ruiyi, Y. Yongqiang, S. Xiulan, Electrochemical aptasensor for detection of acetamiprid in vegetables with graphene aerogel-glutamic acid functionalized graphene quantum dot/gold nanostars as redox probe with catalyst, *Sensor. Actuator. B Chem.* 298 (2019) 126866.
- [139] L. Ma, L. Bai, M. Zhao, J. Zhou, Y. Chen, Z. Mu, An electrochemical aptasensor for highly sensitive detection of zearalenone based on PEI-MoS₂-MWCNTs nanocomposite for signal enhancement, *Anal. Chim. Acta* 1060 (2019) 71–78.
- [140] S.M. Taghdisi, N.M. Danesh, M. Ramezani, A.S. Emrani, K. Abnous, Novel colorimetric aptasensor for zearalenone detection based on nontarget-induced aptamer walker, gold nanoparticles, and exonuclease-assisted recycling amplification, *ACS Appl. Mater. Interfaces* 10 (15) (2018) 12504–12509.
- [141] B. He, X. Yan, A “signal-on” voltammetric aptasensor fabricated by hPt@AuNFs/PEI-rGO and Fe₃O₄NRs/rGO for the detection of zearalenone, *Sensor. Actuator. B Chem.* 290 (2019) 477–483.
- [142] B. He, X. Yan, An amperometric zearalenone aptasensor based on signal amplification by using a composite prepared from porous platinum nanotubes, gold nanoparticles and thionine-labelled graphene oxide, *Microchimica Acta* 186 (6) (2019) 383.
- [143] T. Mushiana, N. Mabuba, A.O. Idris, G.M. Peleyeju, B.O. Orimolade, D. Nkosi, R.F. Ajayi, O.A. Arotiba, An aptasensor for arsenic on a carbon-gold bi-nanoparticle platform, *Sensing and Bio-Sensing Res.* 24 (2019) 100280.
- [144] S. Hassani, M.R. Akmal, A. Salek-Maghsoodi, S. Rahmani, M.R. Ganjali, P. Norouzi, M. Abdollahi, Novel label-free electrochemical aptasensor for determination of Diazinon using gold nanoparticles-modified screen-printed gold electrode, *Biosens. Bioelectron.* 120 (2018) 122–128.
- [145] S. Ramalingam, R. Chand, C.B. Singh, A. Singh, Phosphorene-gold nanocomposite based microfluidic aptasensor for the detection of okadaic acid, *Biosens. Bioelectron.* 135 (2019) 14–21.
- [146] M. Liu, C. Sun, G. Wang, Y. Wang, H. Lu, H. Shi, G. Zhao, A simple, supersensitive and highly selective electrochemical aptasensor for Microcystin-LR based on synergistic signal amplification strategy with graphene, DNase I enzyme and Au nanoparticles, *Electrochim. Acta* 293 (2019) 220–229.
- [147] Q. Wang, X. Qin, L. Geng, Y. Wang, Label-free electrochemical aptasensor for sensitive detection of malachite green based on Au nanoparticle/graphene quantum dots/tungsten disulfide nanocomposites, *Nanomaterials* 9 (2) (2019) 229.
- [148] M. Roushani, A. Nezhadali, Z. Jalilian, An electrochemical chlorpyrifos aptasensor based on the use of a glassy carbon electrode modified with an electropolymerized aptamer-imprinted polymer and gold nanorods, *Microchimica Acta* 185 (12) (2018) 551.
- [149] B. Babamiri, A. Salimi, R. Hallaj, Switchable electrochemiluminescence aptasensor coupled with resonance energy transfer for selective attomolar detection of Hg²⁺ via CdTe@CdS/dendrimer probe and Au nanoparticle quencher, *Biosens. Bioelectron.* 102 (2018) 328–335.
- [150] Y. Gan, J. Sun, T. Liang, J. Tu, N. Hu, H. Wan, P. Wang, An ultrasensitive gold nanoband Aptasensor for mercury (II) detection in aquatic environment, *J. Electrochem. Soc.* 166 (10) (2019) B793–B798.
- [151] Y. Niu, G. Luo, H. Xie, Y. Zhuang, X. Wu, G. Li, W. Sun, Photoelectrochemical aptasensor for lead(II) by exploiting the CdS nanoparticle-assisted photoactivity of TiO₂ nanoparticles and by using the quercetin-copper(II) complex as the DNA intercalator, *Microchimica Acta* 186 (12) (2019) 826.

- [152] J. Ding, Y. Liu, D. Zhang, M. Yu, X. Zhan, D. Zhang, P. Zhou, An electrochemical aptasensor based on gold@polypyrrole composites for detection of lead ions, *Microchimica Acta* 185 (12) (2018) 545.
- [153] C.T. Fakude, O.A. Arotiba, N. Mabuba, Electrochemical aptasensing of cadmium (II) on a carbon black-gold nano-platform, *J. Electroanal. Chem.* 858 (2020) 113796.
- [154] R.L. Lundblad, Development and Application of Biomarkers, CRC Press, 2016.
- [155] S.R. Coughlin, Thrombin signalling and protease-activated receptors, *Nature* 407 (6801) (2000) 258–264.
- [156] L. Yang, X. Zhong, L. Huang, H. Deng, R. Yuan, Y. Yuan, C60@C3N4 nanoparticles as quencher for signal-off photoelectrochemical aptasensor with Au nanoparticle decorated perylene tetracarboxylic acid as platform, *Anal. Chim. Acta* 1077 (2019) 281–287.
- [157] D. Chen, D. Sun, Z. Wang, W. Qin, L. Chen, L. Zhou, Y. Zhang, A DNA nanostructured aptasensor for the sensitive electrochemical detection of HepG2 cells based on multibranch hybridization chain reaction amplification strategy, *Biosens. Bioelectron.* 117 (2018) 416–421.
- [158] N.U. Lin, L.A. Carey, M.C. Liu, J. Younger, S.E. Come, M. Ewend, G.J. Harris, E. Bullitt, A.D. Van den Abbeele, J.W. Henson, Phase II trial of lapatinib for brain metastases in patients with human epidermal growth factor receptor 2-positive breast cancer, *J. Clin. Oncol.: Off. J. Am. Soc. Clin. Oncol.* 26 (12) (2008) 1993.
- [159] S. Albani, L. Maggi, Cytokines as Players of Neuronal Plasticity and Sensitivity to Environment in Healthy and Pathological Brain, *Frontiers Media SA*, 2016.
- [160] M. Hosseini Ghalehno, M. Mirzaei, M. Torkzadeh-Mahani, Electrochemical aptasensor for tumor necrosis factor α using aptamer-antibody sandwich structure and cobalt hexacyanoferrate for signal amplification, *J. Iran. Chem. Soc.* 16 (8) (2019) 1783–1791.
- [161] D.J. Hicklin, L.M. Ellis, Role of the vascular endothelial growth factor pathway in tumor growth and angiogenesis, *J. Clin. Oncol.* 23 (5) (2005) 1011–1027.
- [162] M. Hasanzadeh, N. Shadjou, Advanced nanomaterials for use in electrochemical and optical immunoassays of carcinoembryonic antigen. A review, *Microchimica Acta* 184 (2) (2017) 389–414.
- [163] S. Rose-John, Interleukin-6 family cytokines, *Cold Spring Harbor Perspect. Biol.* 10 (2) (2018) a028415.
- [164] S.C. Yenissetti, L. Phom, A. Mohamad, Dopamine: Health and Disease, (2018) IntechOpen.
- [165] A. Goate, J. Hardy, Twenty years of Alzheimer's disease-causing mutations, *J. Neurochem.* 120 (2012) 3–8.
- [166] K. Blennow, A review of fluid biomarkers for Alzheimer's disease: moving from CSF to blood, *Neurol. Ther.* 6 (1) (2017) 15–24.
- [167] D. Tao, B. Shui, Y. Gu, J. Cheng, W. Zhang, N. Jaffrezic-Renault, S. Song, Z. Guo, Development of a label-free electrochemical aptasensor for the detection of Tau381 and its preliminary application in AD and non-AD patients' sera, *Biosensors* 9 (3) (2019) 84.
- [168] Y. Jiang, D. Sun, Z. Liang, L. Chen, Y. Zhang, Z. Chen, Label-free and competitive aptamer cytosensor based on layer-by-layer assembly of DNA-platinum nanoparticles for ultrasensitive determination of tumor cells, *Sensor. Actuator. B Chem.* 262 (2018) 35–43.
- [169] Y. Zhou, C. Li, X. Li, X. Zhu, B. Ye, M. Xu, A sensitive aptasensor for the detection of β -amyloid oligomers based on metal-organic frameworks as electrochemical signal probes, *Anal. Method.* 10 (36) (2018) 4430–4437.
- [170] Z. Han, M. Luo, Q. Weng, L. Chen, J. Chen, C. Li, Y. Zhou, L. Wang, ZnO flower-rod/g-C3N4-gold nanoparticle-based photoelectrochemical aptasensor for detection of carcinoembryonic antigen, *Anal. Bioanal. Chem.* 410 (25) (2018) 6529–6538.
- [171] X. Zhang, N. Bao, X. Luo, S.-N. Ding, Patchy gold coated Fe3O4 nanospheres with enhanced catalytic activity applied for paper-based bipolar electrode-electrochemiluminescence aptasensors, *Biosens. Bioelectron.* 114 (2018) 44–51.
- [172] J. Li, L. Liu, Y. Ai, Y. Liu, H. Sun, Q. Liang, Self-polymerized dopamine-decorated Au NPs and coordinated with Fe-MOF as a dual binding sites and dual signal-amplifying electrochemical aptasensor for the detection of CEA, *ACS Appl. Mater. Interfaces* 12 (5) (2020) 5500–5510.
- [173] F. Mo, Q. Han, J. Song, J. Wu, P. Ran, Y. Fu, An ultrasensitive "on-off-on" photoelectrochemical thrombin aptasensor based on perylene tetracarboxylic acid/gold nanoparticles/cadmium sulfide quantum dots amplified matrix, *J. Electrochem. Soc.* 165 (14) (2018) B679–B685.
- [174] X. You, W. Lin, H. Wu, Y. Dong, Y. Chi, Carbon dot capped gold nanoflowers for electrochemiluminescent aptasensor of thrombin, *Carbon* 127 (2018) 653–657.
- [175] C. Chen, G. Wei, X. Yao, F. Liao, H. Peng, J. Zhang, N. Hong, L. Cheng, H. Fan, Ru (bpy)₃²⁺/β-cyclodextrin-Au nanoparticles/nanographene functionalized nanocomposites-based thrombin electrochemiluminescence aptasensor, *J. Solid State Electrochem.* 22 (7) (2018) 2059–2066.
- [176] J. Song, S. Li, F. Gao, Q. Wang, Z. Lin, An in situ assembly strategy for the construction of a sensitive and reusable electrochemical aptasensor, *Chem. Commun.* 55 (7) (2019) 905–908.
- [177] Y.-H. Wang, H. Xia, K.-J. Huang, X. Wu, Y.-Y. Ma, R. Deng, Y.-F. Lu, Z.-W. Han, Ultrasensitive determination of thrombin by using an electrode modified with WSe₂ and gold nanoparticles, aptamer-thrombin-aptamer sandwiching, redox cycling, and signal enhancement by alkaline phosphatase, *Microchimica Acta* 185 (11) (2018) 502.
- [178] T. Fan, Y. Du, Y. Yao, J. Wu, S. Meng, J. Luo, X. Zhang, D. Yang, C. Wang, Y. Qian, F. Gao, Rolling circle amplification triggered poly adenine-gold nanoparticles production for label-free electrochemical detection of thrombin, *Sensor. Actuator. B Chem.* 266 (2018) 9–18.
- [179] N. Sattarahmady, A. Rahi, H. Heli, A signal-on built in-marker electrochemical aptasensor for human prostate-specific antigen based on a hairbrush-like gold nanostructure, *Sci. Rep.* 7 (1) (2017) 11238.
- [180] M. Amouzadeh Tabrizi, M. Shamsipur, R. Saber, S. Sarkar, Isolation of HL-60 cancer cells from the human serum sample using MnO₂-PEI/Ni/Au/aptamer as a novel nanomotor and electrochemical determination of thereof by aptamer/gold nanoparticles-poly(3,4-ethylene dioxythiophene) modified GC electrode, *Biosens. Bioelectron.* 110 (2018) 141–146.
- [181] H. Jin, C. Zhao, R. Gui, X. Gao, Z. Wang, Reduced graphene oxide/nile blue/gold nanoparticles complex-modified glassy carbon electrode used as a sensitive and label-free aptasensor for ratiometric electrochemical sensing of dopamine, *Anal. Chim. Acta* 1025 (2018) 154–162.
- [182] D.P. Singh, S.K. Dwivedi, Environmental Microbiology and Biotechnology, New Age International (P) Limited, 2004.
- [183] S. Chen, Y. Frank Cheng, G. Voordouw, Three-dimensional graphene nanosheet doped with gold nanoparticles as electrochemical DNA biosensor for bacterial detection, *Sensor. Actuator. B Chem.* 262 (2018) 860–868.
- [184] A. Dhiman, S. Halder, S.K. Mishra, N. Sharma, A. Bansal, Y. Ahmad, A. Kumar, T.K. Sharma, J.S. Tyagi, Generation and application of DNA aptamers against HspX for accurate diagnosis of tuberculous meningitis, *Tuberculosis* 112 (2018) 27–36.
- [185] R. Das, A. Dhiman, S.K. Mishra, S. Halder, N. Sharma, A. Bansal, Y. Ahmad, A. Kumar, J.S. Tyagi, T.K. Sharma, Structural switching electrochemical DNA aptasensor for the rapid diagnosis of tuberculous meningitis, *Int. J. Nanomed.* 14 (2019) 2103–2113.
- [186] A. Kushwaha, Y. Takamura, K. Nishigaki, M. Biyani, Competitive non-SELEX for the selective and rapid enrichment of DNA aptamers and its use in electrochemical aptasensor, *Sci. Rep.* 9 (1) (2019) 6642.
- [187] C.V.N. HLA, Mycobacterium tuberculosis, *J. Immunol.* 165 (2000) 925–930.
- [188] A.L. Flores-Mireles, J.N. Walker, M. Caparon, S.J. Hultgren, Urinary tract infections: epidemiology, mechanisms of infection and treatment options, *Nat. Rev. Microbiol.* 13 (5) (2015) 269–284.
- [189] K. Reyes, A.C. Bardossy, M. Zervos, Vancomycin-resistant enterococci: epidemiology, infection prevention, and control, *Infect. Dis. Clin.* 30 (4) (2016) 953–965.
- [190] R. Nazari-Vanani, N. Sattarahmady, H. Yadegari, H. Heli, A novel and ultra-sensitive electrochemical DNA biosensor based on an ice crystals-like gold nanostructure for the detection of Enterococcus faecalis gene sequence, *Colloids Surf. B Biointerfaces* 166 (2018) 245–253.
- [191] S. Ranjbar, S. Shahrokhian, Design and fabrication of an electrochemical aptasensor using Au nanoparticles/carbon nanoparticles/cellulose nanofibers nanocomposite for rapid and sensitive detection of Staphylococcus aureus, *Bioelectrochemistry* 123 (2018) 70–76.
- [192] S.S. Zarei, S. Soleimani-Zad, A.A. Ensafi, An impedimetric aptasensor for Shigella dysenteriae using a gold nanoparticle-modified glassy carbon electrode, *Microchimica Acta* 185 (12) (2018) 538.
- [193] S. Ranjbar, S. Shahrokhian, F. Nurmohammadi, Nanoporous gold as a suitable substrate for preparation of a new sensitive electrochemical aptasensor for detection of Salmonella typhimurium, *Sensor. Actuator. B Chem.* 255 (2018) 1536–1544.
- [194] N. Delshadi-Jahromi, R. Nazari-Vanani, H. Yadegari, N. Sattarahmady, G.R. Hatam, H. Heli, Label-free ultrasensitive electrochemical gene sensing of Trichomonas vaginalis using anisotropic-shaped gold nanoparticles as a platform, a repeated sequence of the parasite DNA as a probe, and toluidine blue as a redox marker, *Sensor. Actuator. B Chem.* 273 (2018) 234–241.
- [195] C. Ge, R. Yuan, L. Yi, J. Yang, H. Zhang, L. Li, W. Nian, G. Yi, Target-induced aptamer displacement on gold nanoparticles and rolling circle amplification for ultrasensitive live Salmonella typhimurium electrochemical biosensing, *J. Electroanal. Chem.* 826 (2018) 174–180.